

For reprint orders, please contact [reprints@future-science.com](mailto:reprints@future-science.com)

## Benzoxaboroles: a new class of potential drugs for human African trypanosomiasis

Human African trypanosomiasis, caused by the kinetoplastid parasite *Trypanosoma brucei*, affects thousands of people across sub-Saharan Africa, and is fatal if left untreated. Treatment options for this disease, particularly stage 2 disease, which occurs after parasites have infected brain tissue, are limited due to inadequate efficacy, toxicity and the complexity of treatment regimens. We have discovered and optimized a series of benzoxaborole-6-carboxamides to provide trypanocidal compounds that are orally active in murine models of human African trypanosomiasis. A key feature of this series is the presence of a boron atom in the heterocyclic core structure, which is essential to the observed trypanocidal activity. We also report the *in vivo* pharmacokinetic properties of lead compounds from the series and selection of SCYX-7158 as a preclinical candidate.

Human African trypanosomiasis (HAT), more commonly known as **African sleeping sickness**, is caused by two subspecies of the kinetoplastid parasite *Trypanosoma brucei*, *Trypanosoma brucei gambiense* and *Trypanosoma brucei rhodesiense*, which are introduced into the victim through the bite of the tse-tse fly [1,2]. Endemic across sub-Saharan Africa, tens of thousands of people are infected each year, with millions at risk of contracting the disease [3]. If not treated early in the progression of the disease, the *T. brucei* parasites migrate across the blood–brain barrier and reside in brain tissue, ultimately causing neuronal death leading to a multitude of neurological symptoms including hallucinations, sleep disorders, coma and, ultimately, death [4]. Current treatment options for HAT are inadequate due to lack of efficacy, particularly once the parasites have migrated to the brain (stage 2 HAT), toxicity and the complexity of treatment regimens [5,6]. The most commonly used treatment for stage 2 HAT, melarsoprol (**1**; **FIGURE 1**) is highly toxic, with an estimated 5–10% drug-related mortality. A more recent drug, eflornithine (**2**), while effective against *T.b. gambiense*, is not effective against *T.b. rhodesiense*, and must be administered in a complex intravenous regime that is impractical in disease-endemic areas [7]. Recently, it has been shown that a combination of eflornithine with nifurtimox (**3**), a drug used for Chagas disease that is not effective as a HAT monotherapy, can be effective in a simplified short-course treatment regime, although this still requires multiple infusions of eflornithine [8–11]. Consequently, there is an urgent

need for new drugs to treat HAT and, in particular, a need for a safe, orally active drug that is effective against all known strains of *T. brucei* and is effective in stage 2 HAT.

The creation of boron-containing drugs goes back to the early 1970s when aryl boronic acids were shown to be inhibitors of serine proteases such as subtilisin and chymotrypsin [12]. Due to the unique electronic properties of boron, with its empty p-orbital, these compounds prove to be potent enzyme inhibitors due to their ability to react with a serine hydroxyl in the enzyme active site. These boronic acid inhibitors form a tetrahedral adduct and this moiety serves as a transition-state analog by mimicking the natural transition-state intermediate (**FIGURE 2**).

Over the intervening years, drug researchers have exploited this inherent reactivity of boronic acids and designed inhibitors against a number of therapeutically important enzymes, including thrombin,  $\beta$ -lactamases, HCV protease and dipeptidyl peptidase IV [13–15]. One compound, bortezomib (Velcade<sup>®</sup>), inhibiting the proteasome, has received US FDA approval and is on the market for the treatment of certain cancers.

Anacor Pharmaceuticals was founded in 2002 and employed a novel boron-based chemistry platform to create drug candidates for infectious diseases and inflammatory conditions. Departing from traditional boronic acid chemistry, Anacor focused on creating boron compounds where the boron was incorporated in a ring system fused to an aromatic ring, as exemplified by the 5-fluorobenzoxaborole AN2690 (**4**; **FIGURE 3**), which represents a new class of antifungal drug [16].

**Robert T Jacobs<sup>†</sup>, Jacob J Plattner<sup>2</sup>, Bakela Nare<sup>1</sup>, Stephen A Wring<sup>1</sup>, Daitao Chen<sup>1</sup>, Yvonne Freund<sup>2</sup>, Eric G Gaukel<sup>1</sup>, Matthew D Orr<sup>1</sup>, Joe B Perales<sup>1</sup>, Matthew Jenks<sup>1</sup>, Robert A Noe<sup>1</sup>, Jessica M Sligar<sup>1</sup>, Yong-Kang Zhang<sup>2</sup>, Cyrus J Bacchi<sup>3</sup>, Nigel Yarlett<sup>3</sup> & Robert Don<sup>4</sup>**

<sup>1</sup>SCYNEXIS, Inc., PO Box 12878, Research Triangle Park, NC 27709-2878, USA

<sup>2</sup>Anacor Pharmaceuticals, Inc., 1020 East Meadow Circle, Palo Alto, CA 94303, USA

<sup>3</sup>Haskins Laboratory, Pace University, 41 Park Row, NY 10038, USA

<sup>4</sup>Drugs for Neglected Diseases Initiative, 15 Chemin Louis-Dunant, 1202 Geneva, Switzerland

<sup>†</sup>Author for correspondence:

Tel.: +1 919 544 8600

Fax: +1 919 544 8697

E-mail: [bob.jacobs@scynexis.com](mailto:bob.jacobs@scynexis.com)

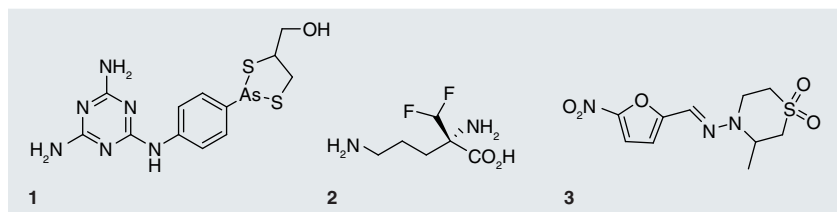


Figure 1. Drugs currently used to treat human African trypanosomiasis.

Analogous to boronic acids, the boron atom in **3** retains the vacant p-orbital and can undergo a reaction with the two hydroxyls on the ribose ring of the terminal tRNA<sup>Leu</sup> adenosine to form an adduct, which is its mechanism for inhibiting cytoplasmic leucyl-tRNA synthetase [17]. Structurally related **benzoxaboroles** (e.g., **5–8**) have also shown selective activity in inhibiting  $\beta$ -lactamases [18], PDE4 [19], bacterial LeuRS [20] and the malaria protozoa [21]. In addition, incorporation of the benzoxaborole scaffold into more complex structures has yielded potent inhibitors of HCV protease [22,23]. In this paper, we describe the discovery of novel benzoxaboroles with antitrypanosomal activity.

## Experimental

### ■ Biological assays

Details of the *in vitro* and *in vivo* assays used to characterize the benzoxaboroles have been described previously [24].

### ■ General laboratory methods

Details of chemical experimental procedures, including chromatographic purification and spectroscopic analysis methods can be found in the **SUPPLEMENTARY DATA**.

### ■ General procedure for preparation of benzoxaborole 6-carboxamides 4-fluoro-*N*-(1-hydroxy-1,3-dihydro-benzo[*c*][1,2]oxaborol-6-yl)-2-trifluoromethylbenzamide (**11**)

A mixture of 6-amino-1-hydroxy-1,2-benzoxaborolane hydrochloride (5 g, 26.9 mmol) and 4-fluoro-2-(trifluoromethyl)-benzoyl chloride (6.1 g, 26.9 mmol) in Et<sub>3</sub>N (11.2 ml, 80.7 mmol) and DCM (200 ml) was allowed to stir overnight

at room temperature. To the reaction was added aqueous hydrochloric acid (100 ml, 1 M), and the mixture was stirred for 1 h. The resulting precipitate was collected by filtration, washed with additional DCM, and dried under vacuum to yield the title compound as an off-white solid (5.2 g, 57%). <sup>1</sup>H NMR (400 MHz, DMSO-d<sub>6</sub>)  $\delta$  ppm 4.96 (s, 2 H) 7.39 (d, *J* = 8.4 Hz, 1 H) 7.61–7.73 (m, 2 H) 7.75–7.87 (m, 2 H) 8.13 (dd, *J* = 1.8, 0.4 Hz, 1 H) 9.25 (s, 1 H) 10.59 (s, 1 H). ESI-MS: [M+H]<sup>+</sup> *m/z* 340. Analysis calculated for C<sub>15</sub>H<sub>10</sub>BF<sub>4</sub>NO<sub>3</sub>: C, 53.14; H, 2.97; N, 4.13. Found: C, 53.18; H, 2.87; N, 4.02.

### *N*-(1-hydroxy-1,3-dihydro-benzo[*c*][1,2]oxaborol-6-yl)-benzenesulfonamide (**15a**)

This compound was prepared as previously reported [25].

### ■ General procedure for preparation of benzoxaborole-6-sulfonamides

#### *N*-(1-hydroxy-1,3-dihydro-benzo[*c*][1,2]oxaborol-6-yl)-4-methylbenzenesulfonamide (**15b**)

A mixture of 6-amino-1-hydroxy-1,2-benzoxaborolane hydrochloride (100 mg, 0.54 mmol), *p*-toluenesulfonyl chloride (130 mg, 0.67 mmol), and pyridine (55  $\mu$ L, 0.67 mmol) in DCM (10 ml) was allowed to stir overnight at room temperature. Aqueous hydrochloric acid (1 M, 3 ml) was added and the resulting mixture was extracted twice with DCM (5 ml). The combined organic phases were dried over sodium sulfate, and the material was concentrated under reduced pressure. The residue was purified by silica-gel chromatography to furnish the title compound as an off white solid. (34 mg, 21%). <sup>1</sup>H NMR (400 MHz, DMSO-d<sub>6</sub>)  $\delta$  2.33 (s, 3 H) 4.88 (s, 2 H) 7.10–7.21 (m, 1 H) 7.22–7.28 (m, 1 H) 7.33 (d, *J* = 7.8 Hz, 2 H) 7.49 (d, *J* = 2.0 Hz, 1 H) 7.62 (d, *J* = 8.4 Hz, 2 H) 9.21 (s, 1 H) 10.17 (s, 1 H). ESI-MS: [M+H]<sup>+</sup> *m/z* 304.

### ■ General procedure for preparation of benzoxaborole-6-ureas

#### 1-(1-hydroxy-1,3-dihydro-benzo[*c*][1,2]oxaborol-6-yl)-3-phenyl urea (**16a**)

A mixture of 6-amino-1-hydroxy-1,2-benzoxaborolane hydrochloride (79 mg, 0.53 mmol) and phenylisocyanate (63 mg, 0.53 mmol) in acetonitrile (10 ml) was allowed to stir overnight at room temperature. The resultant precipitate was collected by vacuum filtration and washed with acetonitrile (30 ml) and diethyl ether (30 ml) to yield the title compound as a

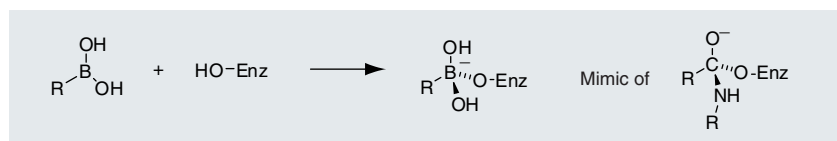


Figure 2. Tetrahedral adduct formation of a boronic acid with an enzyme.

white solid (53 mg, 38%).  $^1\text{H}$  NMR (400 MHz,  $\text{DMSO-d}_6$ )  $\delta$  4.93 (s, 2 H) 6.96 (t,  $J = 7.3$  Hz, 1 H) 7.30 (dd,  $J = 9.7, 8.2$  Hz, 3 H) 7.46 (d,  $J = 7.9$  Hz, 3 H) 7.50–7.61 (m, 1 H) 7.83 (d,  $J = 1.4$  Hz, 1 H) 8.85 (br. s, 2 H) 9.17 (s, 1 H). ESI-MS:  $[\text{M}+\text{H}]^+ m/z$  269.

**(1-hydroxy-1,3-dihydro-benzo[*c*][1,2]oxaborol-6-yl)-carbamic acid *p*-tolyl ester (17b)**

A mixture of 6-amino-1-hydroxy-1,2-benzoxaborolane hydrochloride (100 mg, 0.54 mmol), *p*-tolylchloroformate (77  $\mu\text{L}$ , 0.54 mmol), and triethylamine (0.18 ml, 1.35 mmol) in acetonitrile (10 ml) was allowed to stir overnight at room temperature. The reaction was quenched by slow addition of water (5 ml). The resultant precipitate was collected by vacuum filtration and washed with additional water (10 ml) and dichloromethane (5 ml) to yield the title compound as a white solid (91 mg, 60%).  $^1\text{H}$  NMR (400 MHz,  $\text{DMSO-d}_6$ )  $\delta$  2.31 (s, 3 H) 4.94 (s, 2 H) 7.07–7.14 (m, 3 H) 7.17–7.28 (m, 3 H) 7.35 (d,  $J = 8.4$  Hz, 1 H) 7.58 (dd,  $J = 8.2, 2.1$  Hz, 1 H) 7.88 (d,  $J = 1.6$  Hz, 1 H) 9.21 (s, 1 H) 10.19 (br. s., 1 H). ESI-MS:  $[\text{M}+\text{H}]^+ m/z$  284. Analysis calculated for  $\text{C}_{15}\text{H}_{14}\text{BNO}_4$ : C, 63.64; H, 4.98; N, 4.95. Found: C, 63.77; H, 5.13; N, 4.87.

The following example was prepared by an analogous procedure using 4-methoxyphenyl chloroformate.

**(1-hydroxy-1,3-dihydro-benzo[*c*][1,2]oxaborol-6-yl)-carbamic acid 4-methoxyphenyl ester (17c)**

White solid (29%).  $^1\text{H}$  NMR (400 MHz,  $\text{DMSO-d}_6$ )  $\delta$  3.72 (s, 3 H) 4.90 (s, 2 H) 6.82–7.01 (m, 2 H) 7.02–7.19 (m, 2 H) 7.31 (d,  $J = 8.2$  Hz, 1 H) 7.54 (dd,  $J = 8.2, 2.0$  Hz, 1 H) 7.83 (d,  $J = 1.8$  Hz, 1 H) 9.17 (s, 1 H) 10.13 (br. s., 1 H). ESI-MS:  $[\text{M}+\text{H}]^+ m/z$  300. Analysis calculated for  $\text{C}_{15}\text{H}_{14}\text{BNO}_5$ : C, 60.24; H, 4.72; N, 4.68. Found: C, 60.03; H, 4.78; N, 4.73.

**■ General procedure for preparation of 7-methyl benzoxaborole 6-carboxamides N-(1-hydroxy-7-methyl-1,3-dihydro-benzo[*c*][1,2]oxaborol-6-yl)-benzamide (18a)**

A mixture of 6-amino-7-methyl-3H-benzo[*c*][1,2]oxaborol-1-ol (115 mg, 0.70 mmol) and benzoyl chloride (100  $\mu\text{l}$ , 0.85 mmol) in  $\text{Et}_3\text{N}$  (200  $\mu\text{l}$ , 1.40 mmol) and DCM (10 ml) was allowed to stir overnight at room temperature. To the reaction was added aqueous hydrochloric acid (3 ml, 1M) and the resulting mixture was

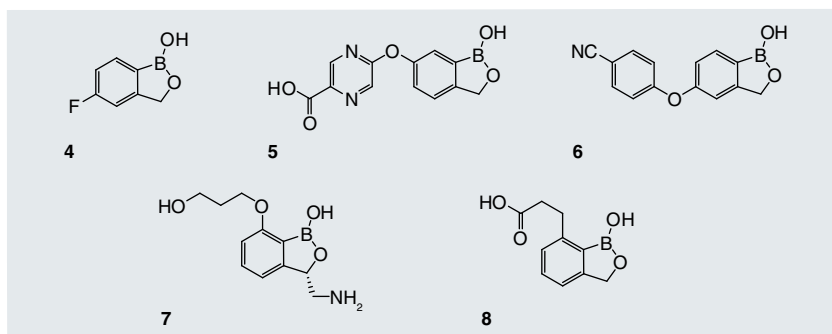


**Figure 3. Benzoxaboroles with anti-infective, anti-inflammatory and antifungal activities.**

extracted twice with DCM (10 ml). The combined organic phases were dried over sodium sulfate, and the material was concentrated under reduced pressure. The residue was purified by silica-gel chromatography to furnish the title compound as a off-white solid (16.2 mg, 8.7%).  $^1\text{H}$  NMR (400 MHz,  $\text{DMSO-d}_6$ )  $\delta$  2.37 (s, 3 H) 4.97 (s, 2 H) 7.23 (d,  $J = 8.0$  Hz, 1 H) 7.40 (d,  $J = 7.8$  Hz, 1 H) 7.45–7.68 (m, 3 H) 7.99 (d,  $J = 7.2$  Hz, 2 H) 9.00 (s, 1 H) 9.89 (s, 1 H). ESI-MS:  $[\text{M}+\text{H}]^+ m/z$  268.

The starting material, 6-amino-7-methyl-3H-benzo[*c*][1,2]oxaborol-1-ol, was prepared as follows:

**(2-bromo-3-methyl-phenyl)-methanol**

2-bromo-3-methyl-benzoic acid (8.2 g, 38.1 mmol) was dissolved in 50 ml of THF.  $\text{BH}_3\text{-THF}$  (76 ml, 76.3 mmol) was added dropwise to the reaction mixture and allowed to stir at room temperature overnight. The reaction was cooled to  $0^\circ\text{C}$  in an ice bath and slowly quenched with MeOH via addition funnel. The solution was then poured into 100-ml saturated  $\text{NaHCO}_3$  and extracted three times with EtOAc. The combined organic phases were dried over sodium sulfate, and the material was concentrated under reduced pressure, which resulted in a white powder (15.2 g, 100%).  $^1\text{H}$  NMR (400 MHz,  $\text{DMSO-d}_6$ )  $\delta$  ppm 2.35 (s, 3 H) 4.51 (s, 2 H) 7.19–7.33 (m, 2 H) 7.33–7.40 (m, 1 H).

**2-(2-bromo-3-methyl-benzyloxy)-tetrahydro-pyran**

To a suspension of (2-bromo-3-methyl-phenyl)-methanol (15.2 g, 76.4 mmol) in DCM (300ml) was added 3,4-dihydro-2H-pyran (14 ml, 152.8 mmol) and camphorsulfonic acid (900 mg). The reaction was allowed to stir at room temperature overnight at which

**Key Terms**

**African sleeping sickness:**

Common name for the disease caused by *Trypanosoma brucei*, which is fatal if untreated and for which suboptimal treatment options exist.

**Benzoxaboroles:** Series of heterocycles containing a boron atom in a five-membered ring adjacent to oxygen fused to a six-membered aromatic ring.

point  $\text{NaHCO}_3$  (900 mg) and  $\text{H}_2\text{O}$  (300 ml) were added. The crude mixture was extracted three times with DCM. The combined organic phases were dried over sodium sulfate, and the material was concentrated under reduced pressure. The residue was purified by silica-gel chromatography to furnish the title compound as a clear oil (20.3 mg, 94%). ESI-MS:  $[\text{M}+\text{H}]^+$   $m/z$  285.

#### 7-methyl-3H-benzo[c][1,2]oxaborol-1-ol

To a cooled ( $-75^\circ\text{C}$ ) solution of 2-(2-bromo-3-methyl-benzyloxy)-tetrahydro-pyran (10 g, 35.2 mmol) in anhydrous THF (200 ml) was added a solution of *n*-butyl lithium (15.5 ml, [2.5 M], 38.7 mmol) in hexanes over 30 min so that the internal temperature remained below  $-65^\circ\text{C}$ . After complete addition of the butyl lithium a white suspension was observed and the internal temperature was maintained between  $-78$  and  $-65^\circ\text{C}$  for an additional hour before a bolus addition of triisopropyl borate (12.2 ml, 52.8 mmol) was added. The reaction mixture was allowed to gradually warm to room temperature overnight before the reaction was quenched with aqueous HCl (40 ml, [6.0 M]). The biphasic mixture was stirred at room temperature for 30 min, then the organic layer was separated. The remaining aqueous layer was extracted with EtOAc ( $3 \times 50$  ml). The combined organic fractions were washed with 1-M NaOH  $1 \times 30$  ml, brine  $1 \times 30$  ml, dried over  $\text{Na}_2\text{SO}_4$ , filtered and concentrated to give 7-methyl-3H-benzo[c][1,2]oxaborol-1-ol (3.7 g, 72%) as a white solid.  $^1\text{H}$  NMR (400 MHz,  $\text{DMSO-d}_6$ )  $\delta$  ppm 2.44 (s, 3 H) 4.94 (s, 2 H) 7.09 (d,  $J = 7.2$  Hz, 1 H) 7.17 (d,  $J = 7.4$  Hz, 1 H) 7.29–7.37 (m, 1 H) 8.89 (br. s, 1 H). ESI-MS:  $[\text{M}+\text{H}]^+$   $m/z$  149.

#### 7-methyl-6-nitro-3H-benzo[c][1,2]oxaborol-1-ol

To 35 ml of fuming  $\text{HNO}_3$  at  $-45^\circ\text{C}$ , 7-methyl-3H-benzo[c][1,2]oxaborol-1-ol (2.5 g, 16.9 mmol) was added in portions over a period of 15 min. The solution was allowed to stir at this temperature for an additional 45 min. The reaction mixture was slowly poured into 200 ml of ice water. The resulting precipitate was collected and dried overnight under vacuum. 7-methyl-6-nitro-3H-benzo[c][1,2]oxaborol-1-ol was recovered as a white solid (1.6 g, 50%).  $^1\text{H}$  NMR (400 MHz,  $\text{DMSO-d}_6$ )  $\delta$  ppm 2.65 (s, 3H) 5.04 (s, 2H) 7.45 (d,  $J = 8.4$  Hz, 1 H) 8.04 (d,  $J = 8.2$  Hz, 1 H) 9.40 (s, 1 H).

#### 6-amino-7-methyl-3H-benzo[c][1,2]oxaborol-1-ol

7-methyl-6-nitro-3H-benzo[c][1,2]oxaborol-1-ol (1.0 g, 5.2 mmol) was dissolved in THF (50 ml). The solution was vacuum degassed and purged with nitrogen, and then palladium (5% on carbon, 275 mg) was added. The reaction was evacuated, charged with hydrogen (1 atm), and then allowed to stir at room temperature overnight. The reaction mixture was filtered through celite and the filtrate was evaporated to dryness. 6-amino-7-methyl-3H-benzo[c][1,2]oxaborol-1-ol was recovered as an off white solid (840 mg, 100%).  $^1\text{H}$  NMR (400 MHz,  $\text{DMSO-d}_6$ )  $\delta$  ppm 2.19 (s, 3 H) 4.80 (s, 2 H) 4.87 (br. s, 2 H) 6.76 (d,  $J = 8.0$  Hz, 1 H) 6.90 (d,  $J = 8.0$  Hz, 1 H) 8.72 (s, 1 H).

#### ■ General procedure for preparation of B-substituted benzoxaborole 6-carboxamides

##### *N*-(1-*p*-Tolyl-1,3-dihydrobenzo[c][1,2]oxaborol-6-yl)-2-trifluoromethylbenzamide (22f)

A 40-ml reaction vessel was charged with a solution of *N*-(1-hydroxy-1,3-dihydrobenzo[c][1,2]oxaborol-6-yl)-2-trifluoromethylbenzamide (9f, 100 mg, 0.31 mmol) in THF (10 ml). The solution was cooled to  $0^\circ\text{C}$  prior to the dropwise addition of *p*-tolyl magnesium bromide (1 M in THF, 1 mmol). The reaction was heated to  $35^\circ\text{C}$  for 2 h, and then allowed to stir at room temperature for an additional 16 h. The reaction was quenched by dropwise addition of aqueous hydrochloric acid (0.5 ml, 1 M), and then concentrated to dryness. The crude residue was purified by silica-gel chromatography (0–10% MeOH in DCM) to furnish the title compound as a white solid (32 mg, 26%).  $^1\text{H}$  NMR (400 MHz, acetone- $d_6$ )  $\delta$  2.40 (s, 3 H) 5.41 (s, 2 H) 7.33 (d,  $J = 7.6$  Hz, 2 H) 7.60 (d,  $J = 8.4$  Hz, 1 H) 7.68–7.77 (m, 1 H) 7.76–7.81 (m, 2 H) 7.85 (d,  $J = 7.8$  Hz, 1 H) 8.02–8.13 (m, 3 H) 8.62 (d,  $J = 1.8$  Hz, 1 H) 9.72 (br. s, 1 H). ESI-MS:  $[\text{M}+\text{H}]^+$   $m/z$  396.

#### ■ General procedure for preparation of 3-methyl benzoxaborole 6-carboxamides

##### 4-fluoro-*N*-(1-hydroxy-3-methyl-1,3-dihydrobenzo[c][1,2]oxaborol-6-yl)-2-trifluoromethyl benzamide (27i)

To a solution of 6-amino-3-methyl-3H-benzo[c][1,2]oxaborol-1-ol acetate salt (102 mg, 0.46 mmol) in DCM (2 ml) was added  $\text{Et}_3\text{N}$  (128.5  $\mu\text{L}$ , 0.92 mmol). The mixture was cooled to  $0^\circ\text{C}$  and the

2-trifluoromethyl-4-fluorobenzoyl chloride (77.0  $\mu$ l, 0.51 mmol) was added slowly via a syringe. The resulting solution was allowed to warm to room temperature gradually and stir for 2 h. The reaction solution was diluted with DCM, washed with 1N HCl, H<sub>2</sub>O and then dried over Na<sub>2</sub>SO<sub>4</sub>, filtered and the filtrate was concentrated under reduced pressure and the crude material was purified by flash chromatography. The title compound **261** was recovered as a white solid (98.3 mg, 61%). <sup>1</sup>H NMR (DMSO-d<sub>6</sub>)  $\delta$ : 10.57 (s, 1H), 9.15 (s, 1H), 8.06 (d, J = 1.8 Hz, 1H), 7.75–7.80 (m, 2H), 7.61–7.70 (m, 2H), 7.35 (d, J = 8.2 Hz, 1H), 5.17 (q, J = 6.5 Hz, 1H), 1.37 (d, J = 6.5 Hz, 3H). ESI-MS: [M+H]<sup>+</sup> *m/z* 354.

The starting material, 6-amino-3-methyl-3H-benzo[c][1,2]oxaborol-1-ol acetate salt, was prepared as follows.

### 3-methyl-3H-benzo[c][1,2]oxaborol-1-ol

Sodium borohydride (941.0 mg, 24.3 mmol 4.0 eq.) was added in portions to a solution of 2-acetylphenylboronic acid (1.00 g, 6.1 mmol) in 3:1 i-PrOH-H<sub>2</sub>O (40 ml). The reaction solution was allowed to stir for 2.5 h at room temperature then the reaction was quenched by dropwise addition of 6M HCl until gas evolution ceased and the reaction mixture reach pH = 1–2. Once the pH was established, the aqueous solution was allowed to stir for an additional 0.5 h. The aqueous solution was then extracted with DCM and the combined DCM extracts were dried over Na<sub>2</sub>SO<sub>4</sub>. The DCM was evaporated and the remaining clear, colorless oil was subjected to SiO<sub>2</sub> chromatography using 3:7 EtOAc–heptane as the eluent. 3-methyl-3H-benzo[c][1,2]oxaborol-1-ol was recovered as clear, colorless, thick oil (741 mg, 82% yield).

### 3-methyl-6-nitro-3H-benzo[c][1,2]oxaborol-1-ol

To fuming HNO<sub>3</sub> (4 ml) at -45°C was added a solution of 3-methyl-3H-benzo[c][1,2]oxaborol-1-ol (616 mg, 4.1 mmol) in nitrobenzene (1 ml) slowly via a syringe while maintaining the reaction temperature between -40 and -45°C. Once the addition was complete the resulting solution was allowed to stir at -45°C for an additional 45 min before poured into crushed ice (20 g). The ice mixture was allowed to melt and the aqueous solution was extracted with dichloromethane. The combined dichloromethane extracts were dried over Na<sub>2</sub>SO<sub>4</sub> then evaporated. The crude oil remaining was

mixed with one liter 1:1 DCM–heptane. The volume of the solution was reduced on a rotovap by half and the resulting solution was allowed to stand overnight in a -20°C freezer overnight. The precipitate formed was filtered out, washed with heptanes and vacuum dried to give 3-methyl-6-nitro-3H-benzo[c][1,2]oxaborol-1-ol as a white solid (612.0 mg, 75% yield). <sup>1</sup>H NMR (DMSO-d<sub>6</sub>)  $\delta$ : 9.49 (br. s, 1H), 8.53 (d, J = 2.2 Hz, 1H), 8.30 (dd, J = 8.4, 2.3 Hz, 1H), 7.67 (d, J = 8.4 Hz, 1H), 5.33 (q, J = 6.7 Hz, 1H), 1.43 (d, J = 6.7 Hz, 3H).

### 6-amino-3-methyl-3H-benzo[c][1,2]oxaborol-1-ol acetate salt

To a solution of 3-methyl-6-nitro-3H-benzo[c][1,2]oxaborol-1-ol (1.33 g, 6.8 mmol) in THF (30 ml) was added HOAc (3.0 ml, 53 mmol). The vessel was vacuum/N<sub>2</sub> purged three times and 5% Pd/C (200 mg) was added. The mixture was again vacuum/N<sub>2</sub> purged three times then vacuum purged again. H<sub>2</sub> was then introduced from a balloon and the reaction was allowed to stir for 2.5 h. The reaction solution was filtered through a short pad of celite and the filtrate was evaporated to yield 6-amino-3-methyl-3H-benzo[c][1,2]oxaborol-1-ol acetate salt as a dark brown foamy solid (1.16 g, 76%). <sup>1</sup>H NMR (DMSO-d<sub>6</sub>)  $\delta$ : 8.79 (s, 1H), 6.99 (d, J = 8.1 Hz, 1H), 6.82 (d, J = 2.0 Hz, 1H), 6.66 (dd, J = 8.1, 2.2 Hz, 1H), 5.02 (q, J = 6.4 Hz, 1H), 4.95 (br. s, 2H), 1.28 (d, J = 6.4 Hz, 3H).

### ■ General procedure for preparation of 3,3-dimethyl benzoxaborole

#### 6-carboxamides

#### 4-fluoro-N-(1-hydroxy-3,3-dimethyl-1,3-dihydro-benzo[c][1,2]oxaborol-6-yl)-2-trifluoromethyl benzamide (**281**)

To a solution of 6-amino-3,3-dimethyl-3H-benzo[c][1,2]oxaborol-1-ol acetate salt (100 mg, 0.42 mmol) in DCM (2 ml) was added Et<sub>3</sub>N (117.3  $\mu$ l, 0.84 mmol). The mixture was cooled to 0°C and the 2-trifluoromethyl-4-fluorobenzoyl chloride (70.0  $\mu$ l, 0.46 mmol) was added slowly via a syringe. The resulting solution was allowed to warm to room temperature gradually and stir for 2 h. The reaction solution was diluted with DCM, washed with 1N HCl, H<sub>2</sub>O and then dried over Na<sub>2</sub>SO<sub>4</sub>, filtered and the filtrate was concentrated under reduced pressure and the crude material was subjected to flash chromatography. The title compound was isolated as a white foam (144.6 mg, 93% yield). <sup>1</sup>H NMR

(DMSO- $d_6$ )  $\delta$ : 10.58 (s, 1H), 9.11 (s, 1H), 8.02 (d,  $J$  = 1.7 Hz, 1H), 7.75–7.83 (m, 2H), 7.60–7.71 (m, 2H), 7.38 (d,  $J$  = 8.2 Hz, 1H), 1.44 (s, 6H). ESI-MS:  $[M+H]^+ m/z$  368.

The starting material, 6-amino-3,3-dimethyl-3H-benzo[*c*][1,2]oxaborol-1-ol acetate salt, was prepared as follows:

#### 2-(2'-bromophenyl)-6-butyl[1,3,6,2]dioxazaborocan

To a suspension of 2-bromophenylboronic acid (10.0g, 49.7 mmol) in toluene (70 ml) was added *N*-butyldiethanolamine (8.5 ml, 52.2 mmol, 1.05 equivalent) via a syringe. The mixture was heated at 50°C for 2 h. After cooling to room temperature, the toluene was evaporated under reduced pressure and the remaining clear colorless crude oil was treated with heptanes (~500 ml). The heptanes mixture was then sonicated for approximately 5 min and the resulting suspension was allowed to stand at room temperature overnight. The solid that precipitated was collected by filtration, washed with heptanes, and dried in a vacuum oven overnight to yield 2-(2'-bromophenyl)-6-butyl[1,3,6,2]dioxazaborocan as a white solid (16.0 g, 98% yield).  $^1H$  NMR (400 MHz,  $CDCl_3$ )  $\delta$  0.86 (t,  $J$  = 7.4 Hz, 3 H) 1.14–1.25 (m, 2 H) 1.51–1.62 (m, 2 H) 2.61–2.70 (m, 2 H) 3.01–3.11 (m, 2 H) 3.26–3.37 (m, 2 H) 4.09–4.26 (m, 4 H) 7.10 (td,  $J$  = 7.6, 2.0 Hz, 1 H) 7.24 (td,  $J$  = 7.3, 1.1 Hz, 1 H) 7.51 (d,  $J$  = 7.9 Hz, 1 H) 7.81 (dd,  $J$  = 7.4, 1.9 Hz, 1 H).

#### 3,3-dimethyl-3H-benzo[*c*][1,2]oxaborol-1-ol

To a solution of 2-(2'-bromophenyl)-6-butyl[1,3,6,2]dioxazaborocan (3.0g, 9.2 mmol) in THF (76 ml) at -78°C was added *n*-BuLi (4.4 ml, 2.5M in hexane, 11.0 mmol, 1.2 equivalent) dropwise via a syringe over a period of 10 min while maintaining reaction temperature at -78°C. After the addition the reaction solution was stirred 20 min at -78°C before acetone (946  $\mu$ l, 12.8 mmol, 1.4 equivalent) was added dropwise via a syringe over a period of 10 min while maintaining the reaction temperature at -78°C. The resulting mixture was allowed to stir for 20 min at -78°C then warm to room temperature gradually. Once the reaction vessel reached room temperature, 6M HCl solution (30 ml) was added and the mixture was stirred for 30 min. The mixture was extracted with EtOAc (three times). The EtOAc extracts were dried over  $Na_2SO_4$ , filtered and concentrated under reduced pressure. The crude, slightly

yellow in color, residual oil remaining was then subjected to flash chromatography to afford 3,3-dimethyl-3H-benzo[*c*][1,2]oxaborol-1-ol as clear colorless oil (1.76 g, 61%).  $^1H$  NMR (400 MHz, DMSO- $d_6$ )  $\delta$  ppm 1.44 (s, 6 H) 7.31 (d,  $J$  = 1.1 Hz, 1 H) 7.38–7.47 (m, 2 H) 7.66 (d,  $J$  = 7.2 Hz, 1 H) 8.99 (s, 1 H).

#### 3,3-dimethyl-6-nitro-3H-benzo[*c*][1,2]oxaborol-1-ol

To 14.2-ml fuming  $HNO_3$  at -45°C was added a solution of 3,3-dimethyl-3H-benzo[*c*][1,2]oxaborol-1-ol (2.28 g, 14.1 mmol) in nitrobenzene (3 ml) slowly via a syringe while maintaining the reaction temperature between -40 and -45°C. Once the addition was complete the resulting solution was allowed to stir at -45°C for an additional 45 min before poured into crushed ice (600 g). The ice mixture was allowed to melt and the aqueous solution was extracted with dichloromethane. The combined dichloromethane extracts were dried over  $Na_2SO_4$  then evaporated. The crude oil remaining was mixed with 1 | 1:1 DCM–heptane. The volume of the solution was reduced on a rotovap by half and the resulting solution was allowed to stand overnight in a -20°C freezer overnight. The precipitate formed was filtered, washed with heptanes and vacuum dried to give 3,3-dimethyl-6-nitro-3H-benzo[*c*][1,2]oxaborol-1-ol as a light yellow solid (2.01 g, 68%).  $^1H$  NMR (400 MHz, DMSO- $d_6$ )  $\delta$  ppm 1.46 (s, 6 H) 7.69 (d,  $J$  = 8.4 Hz, 1 H) 8.28 (dd,  $J$  = 8.4, 2.3 Hz, 1 H) 8.48 (d,  $J$  = 2.2 Hz, 1 H) 9.41 (br. s., 1 H).

#### 6-amino-3,3-dimethyl-3H-benzo[*c*][1,2]oxaborol-1-ol acetate salt

To a solution of 3,3-dimethyl-6-nitro-3H-benzo[*c*][1,2]oxaborol-1-ol (790 mg, 3.8 mmol) in THF (20 ml) was added HOAc (1.7 ml, 30 mmol). The vessel was vacuum/ $N_2$  purged three times and 5% Pd/C (200 mg) was added. The mixture was again vacuum/ $N_2$  purged three times then vacuum purged again.  $H_2$  was then introduced from a balloon and the reaction was allowed to stir for 2.5 h. The reaction solution was filtered through a short pad of celite and the filtrate was evaporated to yield 6-amino-3,3-dimethyl-3H-benzo[*c*][1,2]oxaborol-1-ol acetate salt as a dark brown foamy solid (670 mg, 89%).  $^1H$  NMR (400 MHz, DMSO- $d_6$ )  $\delta$  ppm 1.36 (s, 6 H) 4.94 (s, 2 H) 6.66 (dd,  $J$  = 8.1, 2.2 Hz, 1 H) 6.79 (d,  $J$  = 2.0 Hz, 1 H) 7.01 (d,  $J$  = 8.1 Hz, 1 H) 8.72 (s, 1 H).

***N*-(3-cyclopentyl-1-hydroxy-1,3-dihydro-benzo[*c*][1,2]oxaborol-6-yl)-2-trifluoromethylbenzamide (29f)**

To a solution of 6-amino-3-cyclopentyl-3H-benzo[*c*][1,2]oxaborol-1-ol acetate salt (86.8 mg, 0.4 mmol) in DCM (10 ml) was added Et<sub>3</sub>N (220 μl, 1.6 mmol). The mixture was cooled to 0°C and 2-trifluoromethylbenzoyl chloride (64.6 μl, 0.44 mmol) was added slowly via a syringe. The resulting solution was allowed to warm to room temperature gradually and stir overnight. The reaction solution was diluted with DCM, washed with 1N HCl, H<sub>2</sub>O and then dried over Na<sub>2</sub>SO<sub>4</sub>, filtered and the filtrate was concentrated under reduced pressure and the crude material was subjected to flash chromatography to give the title compound as a white solid. <sup>1</sup>H NMR (acetone-d<sub>6</sub>) δ ppm 9.59 (br. s, 1H), 8.17 (d, J = 1.9 Hz, 1H), 7.78–7.90 (m, 2H), 7.74–7.76 (m, 2H), 7.66–7.72 (m, 2H), 7.39 (d, J = 8.2 Hz, 1H), 5.13 (d, J = 4.8 Hz, 1H), 2.31 (td, J = 8.2, 4.8 Hz, 1H), 1.81–1.93 (m, 1H), 1.60–1.75 (m, 2H), 1.42–1.60 (m, 3H), 1.29–1.41 (m, 1H), 1.08–1.22 (m, 1H). ESI-MS: [M+H]<sup>+</sup> *m/z* 390.

The starting material, 6-amino-3-cyclopentyl-3H-benzo[*c*][1,2]oxaborol-1-ol acetate salt, was prepared as follows.

**2-(2'-formylphenyl)-6-butyl[1,3,6,2]dioxazaborocan**

To a suspension of 2-formylphenylboronic acid (4.5 g, 30.0 mmol) in toluene (40 ml) was added *N*-butyldiethanolamine (5.2 ml, 31.5 mmol, 1.05 equiv.) via a syringe. The mixture was heated at 50°C for 2 h. After cooling to room temperature, the toluene was and the remaining yellow oil was treated with heptanes (50 ml) and the mixture was again evaporated under reduced pressure. The resulting yellow solid was crashed into small pieces and washed with heptanes to give 2-(2'-formylphenyl)-6-butyl[1,3,6,2]dioxazaborocan as a white powder (9.0 g, 100% yield). <sup>1</sup>H NMR (CDCl<sub>3</sub>) δ: 10.92 (s, 1H), 7.87 (dd, J = 7.7, 1.1 Hz, 1H), 7.83 (d, J = 7.5 Hz, 1H), 7.48 (td, J = 7.4, 1.3 Hz, 1H), 7.33–7.40 (m, 1H), 4.03–4.26 (m, 4H), 3.07–3.14 (m, 4H), 2.23–2.36 (m, 2H), 1.41–1.54 (m, 2H), 1.00–1.15 (m, 2H), 0.77 (t, J = 7.3 Hz, 3H).

**3-cyclopentyl-3H-benzo[*c*][1,2]oxaborol-1-ol**

To a solution of 2-(2'-formylphenyl)-6-butyl[1,3,6,2]dioxazaborocan (5.0 g, 18.1 mmol) in THF (100 ml) at -45°C was added cyclopentyl magnesium bromide (9.1-ml, 2.0-M solution in

THF, 18.1 mmol) via a syringe. The mixture was allowed to warm to room temperature gradually over 1 h before being quenched with HCl (20 ml, 6N). The acidic mixture was stirred for 1 h and was extracted with EtOAc (three times). Combined organics was washed with H<sub>2</sub>O, brine, dried over Na<sub>2</sub>SO<sub>4</sub>, filtered and the filtrate was concentrated under reduced pressure. The residue was purified by flash chromatography to give 3-cyclopentyl-3H-benzo[*c*][1,2]oxaborol-1-ol as a colorless oil. <sup>1</sup>H NMR (DMSO-d<sub>6</sub>) δ: 9.07 (s, 1H), 7.69 (d, J = 7.2 Hz, 1H), 7.37–7.47 (m, 2H), 7.28–7.36 (m, 1H), 5.12 (d, J = 4.7 Hz, 1H), 2.27 (td, J = 8.2, 4.9 Hz, 1H), 1.78–1.90 (m, 1H), 1.56–1.74 (m, 3H), 1.39–1.56 (m, 4H), 1.20–1.34 (m, 1H).

**3-cyclopentyl-6-nitro-3H-benzo[*c*][1,2]oxaborol-1-ol**

To fuming HNO<sub>3</sub> (20 ml) at -45°C was added a solution of 3-cyclopentyl-3H-benzo[*c*][1,2]oxaborol-1-ol (1.4 g, 7.0 mmol) in nitrobenzene (3 ml) slowly via a syringe while maintaining the reaction temperature between -40 to -45°C. Once the addition was complete the resulting solution was allowed to stir at -45°C for an additional 45 min before poured into crushed ice (60 g). The ice mixture was allowed to warm to room temperature and the precipitate formed was filtered, washed with heptanes and vacuum dried to give 3-cyclopentyl-6-nitro-3H-benzo[*c*][1,2]oxaborol-1-ol as a light yellow solid. <sup>1</sup>H NMR (DMSO-d<sub>6</sub>) δ: 9.53 (s, 1H), 8.55 (d, J = 2.2 Hz, 1H), 8.32 (dd, J = 8.4, 2.3 Hz, 1H), 7.70 (d, J = 8.5 Hz, 1H), 5.29 (d, J = 4.6 Hz, 1H), 2.31–2.42 (m, 1H), 1.80–1.92 (m, 1H), 1.57–1.71 (m, 2H), 1.38–1.57 (m, 3H), 1.17–1.30 (m, 1H), 0.93–1.06 (m, 1H).

**6-amino-3-cyclopentyl-3H-benzo[*c*][1,2]oxaborol-1-ol acetate salt**

To a solution of 3-cyclopentyl-6-nitro-3H-benzo[*c*][1,2]oxaborol-1-ol (970 mg, 3.9 mmol) in THF (20 ml) was added HOAc (2.0 ml, 33 mmol). The vessel was vacuum/N<sub>2</sub> purged three times and 5% Pd/C (200 mg) was added. The mixture was again vacuum/N<sub>2</sub> purged three times then vacuum purged again. Hydrogen was then introduced from a balloon and the reaction was allowed to stir for 2.5 h. The reaction solution was filtered through a short pad of diatomaceous earth and the filtrate was evaporated to yield 6-amino-3-cyclopentyl-3H-benzo[*c*][1,2]oxaborol-1-ol acetate salt as a dark brown foamy solid.

*N*-(1-hydroxy-3-isobutyl-1,3-dihydro-benzo[*c*][1,2]oxaborol-6-yl)-2-trifluoromethylbenzamide (**30f**)

Compound **30f** was prepared using a procedure similar to that of **29f**, except starting with 6-amino-3-isobutyl-3H-benzo[*c*][1,2]oxaborol-1-ol acetate, prepared analogously to the cyclopentyl analog described above, except using isobutylmagnesium bromide in place of cyclopentylmagnesium bromide in the second step. Data for compound **29f**:  $^1\text{H NMR}$  (DMSO- $d_6$ )  $\delta$ : 10.53 (s, 1H), 9.13 (s, 1H), 8.06 (d,  $J = 1.9$  Hz, 1H), 7.81 (d,  $J = 7.5$  Hz, 1H), 7.73–7.79 (m, 1H), 7.65–7.71 (m, 2H), 7.62 (dd,  $J = 8.2, 2.0$  Hz, 1H), 7.31 (d,  $J = 8.2$  Hz, 1H), 5.10 (dd,  $J = 9.8, 3.0$  Hz, 1H), 1.81–1.92 (m, 1H), 1.65 (ddd,  $J = 13.9, 9.0, 3.1$  Hz, 1H), 1.27 (ddd,  $J = 14.1, 9.7, 4.6$  Hz, 1H), 0.98 (d,  $J = 6.6$  Hz, 3H), 0.89 (d,  $J = 6.7$  Hz, 3H). ESI-MS:  $[\text{M}+\text{H}]^+ m/z$  378.

## Results & discussion

### Discovery of benzoxaboroles as antitrypanosomal agents

Focused screening of the Anacor chemical library in a whole-cell trypanocidal assay identified a number of benzoxaboroles as potential starting points for a medicinal chemistry lead-identification and optimization program. Early structure–activity relationships (SAR) gleaned from compounds available in the existing chemical library suggested that benzoxaboroles containing a substituent at C(6) of the heterocyclic ring system (e.g., **9–11**; **FIGURE 4**) were particularly interesting [25]. While initial optimization efforts focused on the 6-S series, exemplified by the 4-chlorophenyl sulfoxide analog AN2920 (**8a**), delivered analogs with good *in vitro* trypanocidal activity, *in vivo* activity in a mouse model of non-CNS stage 1 HAT was modest.

Synthetic challenges encountered in the 6-S series prompted us to focus our attention on the 6-N series exemplified by AN2951 (**11a**). In addition to the unsubstituted benzamide, several substituted benzamides were available from the library, which demonstrated that variation of electronic properties of substituent(s) had

little effect on *in vitro* potency, as summarized in **TABLE 1**. In contrast, the *in vitro* metabolic stability of these benzamides were more heavily impacted by the choice of substituent, with several analogs (**11e**, **11f** (AN3520)) exhibiting good metabolic stability in a mouse S9 liver fraction assay. Encouragingly, aqueous solubility and lipophilicity (logD) were within generally acceptable ranges predictive of oral availability [26,27]. Permeability across the blood–brain barrier was predicted to be good, with little predicted interaction with the P-glycoprotein (Pgp)-efflux transporter, based on the MDCK-MDR1 cell monolayer assay [28,29]. Further development of SAR of the benzamide region afforded compound **111** (SCYX-6759), which was selected for further characterization in an array of *in vitro* and *in vivo* experiments [24].

To explore the importance of the presence of the boron atom for antiparasitic activity, we prepared the lactone analogs of (**12a**) and (**12f**) (**FIGURE 5**). These analogs were completely inactive in the whole-cell *T. brucei* assay at the highest concentration tested (30  $\mu\text{M}$ ). Furthermore, the acyclic arylboronic acids **13** and **14**, analogs of trypanocidal oxaboroles (**11a** & **15a**, respectively) were similarly inactive in the *in vitro* *T. brucei* assay.

### Variation of 6-N linker: sulfonamides, ureas & urethanes

One of the regions explored in the benzoxaborole series was the linker between the heterocyclic core and pendant aryl group. When the carboxamide was replaced by sulfonamide (**15**), *in vitro* potency versus *T. brucei* was maintained, but cytotoxicity to mammalian cells was observed (**TABLE 2**). Ureas (**16**) were next explored, where we found that potency in the whole-cell *T. brucei* assay was comparable to that observed for the corresponding carboxamides, and cytotoxicity was generally low. We also briefly explored aryl carbamate analogs (**17a** & **17b**), but quickly discovered that these compounds were significantly less active, and also suffered from chemical instability.

As observed in the carboxamides, metabolic stability of the sulfonamides and ureas was determined to a large degree by the presence and nature of substituents on the pendant aryl ring, with 4-substituted analogs (**15b** & **15c**) generally exhibiting improved stability. When evaluated in the *in vitro* MDCK-MDR1 permeability assay, some evidence for interaction with the Pgp efflux transporter was observed

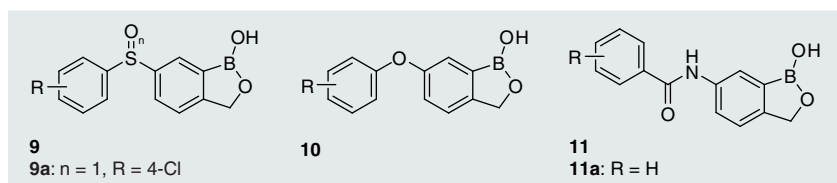


**Figure 4.** Substituted benzoxaboroles identified in a trypanocidal screening effort.

for the aryl sulfonamides, particularly in the 4-methoxyphenyl analog (**15b**). In contrast, the electron-deficient 4-chlorophenyl analog (**15n**) exhibited high permeability and low propensity for Pgp efflux. Predicted permeability of the ureas was also low, as early examples (e.g., **16a** & **16c**) exhibited low apparent permeability values in the MDR1-MDCK assay, and some examples (**16j** & **16o**) exhibited modest propensity for Pgp efflux. Aqueous solubility was generally poor for the urea analogs examined. Taken together, the lack of significant improvement in the *in vitro* potency coupled with the deleterious effects on cytotoxicity, physicochemical and *in vitro* ADME properties observed for these alternative linker moieties prompted us to focus the majority of our subsequent effort in the benzamide series.

#### ■ Substituents on the benzoxaborole ring in 6-carboxamides

Given the relative insensitivity of trypanocidal activity to modification of the benzamide region and the limitations on *in vitro* ADME properties observed in alternative linker functionalities, we sought to improve activity through introduction of substituents on the benzoxaborole core.

Access to compounds substituted at C(5) or C(7) was limited due to the relatively capricious nature of the nitration/hydrogenation sequence that installed the C(6) substituent when substituents were present at C(5) or C(7). For example, when an electron-donating substituent such as methoxy was introduced at C(5), the nitration proceeded well, but hydrogenation to the corresponding aniline was accompanied by extensive decomposition of the product prior to acylation. In contrast, nitration of the 5-fluoro benzoxaborole resulted in a complex mixture of products from which the desired 6-nitro compound could be isolated only in very low yield. Nitration of the 7-fluoro oxaborole predominantly delivered the 4-nitro isomer, with the 6-nitro present as less than 20% of the crude reaction mixture. Greater success was found in the C(7)-methyl series, where both nitration and hydrogenation proceeded with reasonable efficiency, as summarized in **TABLE 3**. Interestingly, the SAR of the C(7)-methyl analogs did not parallel that observed in the unsubstituted oxaboroles. Specifically, where we had observed that incorporation of an electron withdrawing substituent (Cl or CF<sub>3</sub>) at the *ortho* position of the benzamide was beneficial in the unsubstituted oxaboroles,

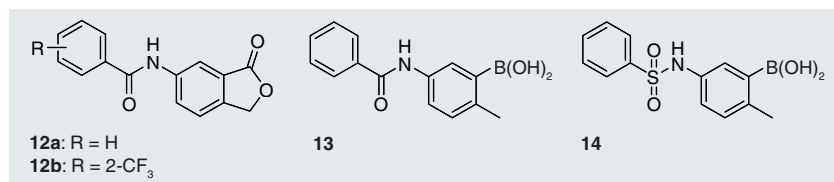


**Figure 5. Nonbenzoxaborole analogs evaluated for trypanocidal activity.**

the corresponding C(7) analogs (e.g., **18h**, **18l** & **18m**) were less potent than either the unsubstituted (**18a**) or 4-substituted (**18b** & **18n**) derivatives.

#### ■ Substitution of the benzoxaborole heterocyclic ring

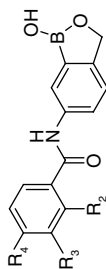
The final area of the benzoxaborole ring system that was explored to improve efficacy was the five-membered oxaborole heterocycle. Specifically, two strategies were explored: introduction of substituents on the boron atom and introduction of substituents at C(3).

#### B-substituted oxaborole-6-carboxamides

It was found that reaction of a benzoxaborole 6-carboxamide with a Grignard reagent proceeded with good efficiency to provide the corresponding B-alkyl or B-aryl analog. The B-methyl (**19f**) and B-vinyl (**20f**) analogs of **11f** were found to be cytotoxic, whereas the B-phenyl (**21f**) analog was not; therefore, effort focused on the B-aryl series (**TABLE 4**).

Several trends were noted in the SAR of initial compounds in the B-aryl series. Potency in the *in vitro* assay appeared to be directly related to the electronic density on the B-aryl ring, with electron-rich systems such as the 4-methoxyphenyl (**24f**), 4-dimethylaminophenyl (**25f**) and 3,4-dimethoxyphenyl (**26f**) analogs exhibiting the greatest potency. Conversely, metabolic stability was greatest in compounds bearing electron-deficient B-aryl rings such as 4-chlorophenyl (**23f**). These SAR trends prompted us to consider the possibility that the B-aryl compounds were efficacious not only due to their intrinsic trypanocidal activity, but might also be converted to the corresponding parent oxaborole via an oxidative cleavage of the B-aryl bond. While we could not find conclusive evidence of this metabolism occurring in the *in vitro* assay, we were able to demonstrate that oxidative de-arylation was significant when a B-aryl compound (**24i**) was dosed to mice, as both the parent and de-arylated analog (**11i**) were observed in mouse plasma.

Table 1. Structure–activity relationship of substituted benzamides.



Compound	R2	R3	R4	TBB IC <sub>50</sub> (μg/ml) <sup>†</sup>	L929 IC <sub>50</sub> (μg/ml) <sup>‡</sup>	Mouse S9 metabolism (t <sub>1/2</sub> , min) <sup>§</sup>	logD	Solubility (μM)¶	Permeability <sup>#</sup>		<i>In vivo</i> , acute HAT model**
									P <sub>app</sub> (nm/s)	P <sub>app</sub> +918 (nm/s)	
IIa	H	H	H	0.04	>10	29		640	697	0.08	
IIb	H	H	CF <sub>3</sub>	0.03	>10	15	2.55	100	660	0.0	
IIc	H	H	OCH <sub>3</sub>	0.02	>10	96	2.21	>200	648	0.01	ip (+), po (-)
IId	H	H	F	0.07	>10	69	2.27	>200	625	0.03	ip (+), po (+)
IIe	H	H	CF <sub>3</sub>	0.06	>10	>350	3.54	50	438	0.01	po (+++)
IIf	CF <sub>3</sub>	H	H	0.04	3.77	>350	2.25	>200	430	0.02	ip (+), po (+++)
IIg	F	H	H	0.03	>10	62	2.03	>200	459	-0.02	po (-)
IIh	Cl	H	H	0.03	>10	67	2.00	100	569	-0.06	po (+++)
IIIi	H	F	H	0.05	>10	69		531	494	-0.08	
IIIj	H	Cl	H	0.04	>10	119	2.83	50	490	-0.08	po (-)
IIIk	H	CF <sub>3</sub>	H	0.05	>10	104	3.38	100	469	-0.08	po (-)
IIIl	CF <sub>3</sub>	H	F	0.05	>10	>350	2.57	>200	379	0.02	po (+++)
III m	Cl	H	F	0.04	>10	>350	2.23	25	670	-0.07	po (+++)

(+++)= active at 5 mg/kg; (++)= active at 10 mg/kg; (+)= active at 20 mg/kg; (-)= inactive at 20 mg/kg.

<sup>†</sup>Trypanocidal activity versus Trypanosoma brucei EATRO 110 parasites [32].

<sup>‡</sup>Cytotoxicity versus L929 mouse fibroblasts.

<sup>§</sup>Stability in mouse S9 liver fraction.

<sup>¶</sup>Solubility in pH 7.4 PBS.

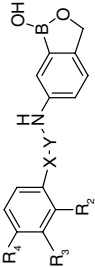
<sup>#</sup>Permeability in an MDCK-MDR1 cell monolayer assay.

<sup>††</sup>[29].

\*\*Activity in a stage 1 HAT model using mice infected with T. brucei EATRO 110 parasites [32].

AQ: Absorption quotient; HAT: Human African trypanosomiasis; ip: intraperitoneal dosing; P<sub>app</sub>: Apparent permeability; po: per os (oral) dosing; TBB: T. b. brucei.

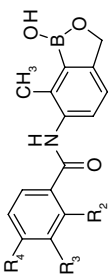
Table 2. Structure-activity relationship of substituted sulfonamides, ureas and carbamates.



Compound	R2	R3	R4	X-Y	TBB IC <sub>50</sub> <sup>†</sup> (μg/ml) <sup>†</sup>	L929 IC <sub>50</sub> <sup>‡</sup> (μg/ml) <sup>‡</sup>	Mouse S9 metabolism (t <sub>1/2</sub> , min) <sup>§</sup>	logD	Solubility (μM) <sup>¶</sup>	Permeability <sup>#</sup>		In vivo, acute HAT model <sup>**</sup>
										P <sub>app</sub> (nm/s)	P <sub>app</sub> +918 (nm/s)	
<b>I5a</b>	H	H	H	-SO <sub>2</sub> -	0.02	2.65	28		>200	319	391	0.18
<b>I5b</b>	H	H	CH <sub>3</sub>	-SO <sub>2</sub> -	0.02	2.67	219			286	312	0.08
<b>I5c</b>	H	H	OCH <sub>3</sub>	-SO <sub>2</sub> -	0.03	2.1	>350	1.95		241	334	0.28
<b>I5g</b>	F	H	H	-SO <sub>2</sub> -	0.047	5.88	>350					ip (+), po (-) po (-)
<b>I5n</b>	H	H	Cl	-SO <sub>2</sub> -	0.03	2.6	106			412	447	0.08
<b>I6a</b>	H	H	H	-NHCO-	0.047	>10	30	2.27	50	167	153	-0.09
<b>I6b</b>	H	H	CH <sub>3</sub>	-NHCO-	0.045	>10	40	2.86	13	341	332	0.00
<b>I6c</b>	H	H	OCH <sub>3</sub>	-NHCO-	0.059	>10	178	2.21	25	120	122	0.01
<b>I6f</b>	CF <sub>3</sub>	H	H	-NHCO-	0.155	>10		3.08	25	333	348	0.04
<b>I6g</b>	F	H	H	-NHCO-	0.025	>10	18	2.46	13	313	328	0.05
<b>I6h</b>	Cl	H	H	-NHCO-	0.039	>10	29			664	661	0.00
<b>I6j</b>	H	Cl	H	-NHCO-	0.042	>10	75			159	346	0.54
<b>I6o</b>	H	OCH <sub>3</sub>	H	-NHCO-	0.022	>10	91			140	181	0.23
<b>I7b</b>	H	H	CH <sub>3</sub>	-OCO-	0.566	4.28	25					po (-)
<b>I7c</b>	H	H	OCH <sub>3</sub>	-OCO-	0.565	3.12	64					

(+++)= active at 5 mg/kg; (++)= active at 10 mg/kg; (+)= active at 20 mg/kg; (-)= inactive at 20 mg/kg.  
<sup>†</sup>Trypanocidal activity versus Trypanosoma brucei EATRO 110 parasites [32].  
<sup>‡</sup>Cytotoxicity versus L929 mouse fibroblasts.  
<sup>§</sup>Stability in mouse S9 liver fraction.  
<sup>¶</sup>Solubility in pH 7.4 PBS.  
<sup>#</sup>Permeability in an MDCK-MDR1 cell monolayer assay.  
<sup>\*\*</sup>[29].  
<sup>\*\*</sup>Activity in a stage 1 HAT model using mice infected with T. brucei EATRO 110 parasites [32].  
 AQ: Absorption quotient; HAT: Human African trypanosomiasis; ip: intraperitoneal dosing; P<sub>app</sub>: Apparent permeability; po: per os (oral) dosing; TBB: T. b. brucei.

Table 3. Structure–activity relationship of 7-methyl benzoxaborole derivatives.



Compound	R2'	R3'	R4'	TBB IC <sub>50</sub> (μg/ml) <sup>†</sup>	L929 IC <sub>50</sub> (μg/ml) <sup>‡</sup>	Mouse S9 metabolism (t <sub>1/2</sub> , min) <sup>§</sup>	logD	Solubility (μM) <sup>  </sup>	Permeability <sup>#</sup>		In vivo, acute HAT model <sup>##</sup>
									P <sub>app</sub> (nm/s)	P <sub>app</sub> +918 (nm/s)	
<b>18a</b>	H	H	H	0.364	>10	>350	2.01	>200			
<b>18b</b>	H	H	CH <sub>3</sub>	0.094	>10		2.80	100			
<b>18h</b>	Cl	H	H	0.475	>10						
<b>18j</b>	H	Cl	H	0.556	>10						
<b>18l</b>	CF <sub>3</sub>	H	F	0.28	>10	>350			567	560	-0.01
<b>18m</b>	Cl	H	F	1.26	>10						
<b>18n</b>	H	H	Cl	0.11	>10	233	3.01	100			po (+)
<b>18p</b>	F	H	F	0.097	>10	>350	3.03	100	739	751	0.02

(+++)= active at 5 mg/kg; (++)= active at 10 mg/kg; (+)= active at 20 mg/kg; (-)= inactive at 20 mg/kg.  
<sup>†</sup>Trypanocidal activity versus Trypanosoma brucei brucei S427.  
<sup>‡</sup>Cytotoxicity versus L929 mouse fibroblasts.  
<sup>§</sup>Stability in mouse S9 liver fraction.  
<sup>||</sup>Solubility in pH 7.4 PBS.  
<sup>#</sup>Permeability in an MDCK-MDR1 cell monolayer assay.  
<sup>##</sup>Activity in a stage 1 HAT model using mice infected with T. brucei EATRO 110 parasites [32].  
 AQ: Absorption quotient; HAT: Human African trypanosomiasis; P<sub>app</sub>: Apparent permeability; po: per os (oral) dosing; TBB: T. b. brucei.

## C(3)-substituted benzoxaboroles

Introduction of a methyl group at C(3) of the benzoxaborole ring had little effect on the trypanocidal potency, but a significant increase in cytotoxicity was observed for the majority these analogs (**27h**, **27l** & **27m**; TABLE 5). As initial samples of C(3)-methyl analogs were prepared as racemates, we confirmed that both the trypanocidal activity and cytotoxicity were present in the same stereochemical series by preparation of pure enantiomers of **27l**. Disappointingly, the *R* enantiomer was very potent in both assays, but the *S* enantiomer exhibited some trypanocidal activity while essentially inactive in the cytotoxicity assay. This observation was used to advantage in progression to the C(3)-dimethyl analogs (**28f**, **28h**, **28l** (SCYX-7158) & **28m**), which retained trypanocidal activity but were not cytotoxic. Larger mono-substituted C(3) analogs, such as cyclopentyl (**29f**) and isobutyl (**30f**) were less active. *In vitro* potency against additional *T. brucei* strains.

While our primary *in vitro* assay for assessment of potency employed the widely used and well-characterized *T. b. brucei* S427 strain, we felt that it was important to ensure that the SAR that we developed using this assay translated to human-infective *T. b. rhodesiense* and *T. b. gambiense* strains, including several melarsoprol-resistant strains [30,31]. We were pleased to find that this translation was observed for all of the chemotypes evaluated, as summarized in TABLE 4.

## ■ In vivo pharmacokinetics &amp; efficacy

## In vivo efficacy in stage I HAT model

Concurrent with the exploration of *in vitro* potency, physicochemical and ADME properties, as described earlier, selected compounds from each of the subclasses explored were progressed to a mouse model of stage 1 HAT [32]. To help understand whether metabolism was an important factor for *in vivo* efficacy and pharmacokinetics (PKs) models.

In these initial *in vivo* experiments, the 2-trifluoromethyl benzamide **11f** emerged as a lead compound, as it exhibited good plasma PK and was efficacious in a murine model of stage 1 (non-CNS) HAT. Further exploration of substitution on the benzamide region revealed that installation of a fluoro substituent at C(4) in combination with the C(2) trifluoromethyl group (**11l**) afforded further improvements in

Table 4. Characterization of benzoxaboroles in additional *Trypanosoma brucei* strains.

Compound	<i>Trypanosoma brucei</i> IC <sub>50</sub> (µg/ml)	<i>Trypanosoma brucei rhodesiense</i> IC <sub>50</sub> (µg/ml)	<i>Trypanosoma brucei gambiense</i> IC <sub>50</sub> (µg/ml)				
	S427 strain	STIB 900 strain <sup>†</sup>	108R strain <sup>‡</sup>	40R strain <sup>§</sup>	DAL 1402 strain <sup>  </sup>	DRANI strain <sup>#</sup>	ITMAP 141267 strain <sup>††</sup>
<b>IIa</b>	0.04	0.041	0.046	0.047	0.033	0.062	0.048
<b>IIb</b>	0.03	0.0595	0.06	0.054	0.033	0.059	0.041
<b>IIc</b>	0.02	0.053	0.03	0.035	0.024	0.045	0.028
<b>IId</b>	0.07	0.114					
<b>IIf</b>	0.04	0.037	0.026	0.033	0.011	0.024	0.015
<b>IIh</b>	0.03	0.033	0.018	0.022	0.006	0.016	0.013
<b>III</b>	0.05	0.038	0.033	0.023	0.009	0.018	0.016
<b>IIIm</b>	0.04	0.035	0.017	0.032	0.011	0.019	0.016
<b>I5b</b>	0.02	0.108					
<b>I5c</b>	0.03	<0.02					
<b>I5n</b>	0.03	0.023					
<b>I6a</b>	0.047	0.163					
<b>I6b</b>	0.045	0.1195					
<b>I6c</b>	0.059	0.299					
<b>27I</b>	0.091	0.116	0.07	0.085	0.031	0.065	0.048
<b>28I</b>	0.292	0.294	0.165	0.363	0.065	0.129	0.092
<b>28h</b>	0.282	0.155	0.134	0.109	0.049	0.109	0.069

<sup>†</sup>Isolated from a patient in Tanzania in 1982.

<sup>‡</sup>Isolated from a patient in Democratic Republic of Congo (DRC) in 2005, relapsed 8 months after melarsoprol treatment.

<sup>§</sup>Isolated from a patient in DRC in 2005, relapsed 6 months after melarsoprol treatment.

<sup>||</sup>Isolated from a patient in Cote d'Ivoire in 1990.

<sup>#</sup>Isolated from a patient in Uganda in 1995.

<sup>††</sup>Isolated from a patient in DRC in 1960. All strains were adapted to cell culture at Swiss Tropical and Public Health Institute. For a general description of strains, see [30,31].

*in vivo* PK and efficacy properties [24]. In addition, the 2-chloro (**IIh**) and 2-chloro-4-fluoro (**IIIm**) analogs exhibited comparable *in vivo* efficacy in the stage 1 HAT model.

We were disappointed to find that many of the modifications made to these initial 6-carboxamide leads did not improve *in vivo* efficacy in the stage 1 HAT model. As described earlier, modification of the linker (e.g., sulfonamides and ureas) was accompanied by lower *in vivo* efficacy for representative compounds evaluated in this model, (**I5c**, **I5g**, **I6a** & **I6o**), attributable to a combination of metabolic instability or reduced permeability (**TABLE 2**). The B-aryl series (**TABLE 6**) initially appeared to hold promise for improved permeability, but evaluation of representative compounds (**26f** & **24I**) from this series in the acute *in vivo* model revealed poor potency, and *in vivo* PK studies revealed that metabolism to the parent benzoxaborole by oxidative cleavage of the B-aryl bond was significant.

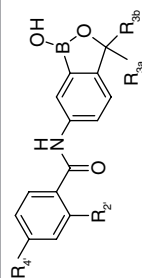
Much greater success in improving overall profile was achieved through exploration of the 3-substituted benzoxaboroles. While the

3-monosubstituted series was compromised to some degree by cytotoxicity, analogs from this series (**27d** & **27h**) were quite active in the stage 1 *in vivo* model. Further improvement in the *in vivo* potency was observed in the 3,3-dimethyl analogs (**28f**, **28h**, **28I** & **28m**), even though these compounds were slightly less potent in the *in vitro* trypanocidal assay. This apparent disconnect between *in vitro* potency and *in vivo* efficacy is most likely explained by the superior PKs of the 3,3-dimethyl analogs (see later discussion). The most interesting compound from this series (**28m**) was able to completely cure animals at a dose of 5 mg/kg in the stage 1 model.

#### *In vivo* efficacy in stage 2 HAT model

As the primary focus of our program was to identify drug candidates for stage 2 HAT, **IIIf**, **IIh** and **III** were evaluated in a murine model of stage 2 HAT [33,34], where they were found to be effective when administered intraperitoneally at a dose of 50 mg/kg twice daily for 14 days, with **III** able to cure 10/10 infected animals (**TABLE 7**, entries 1–3) [24].

Table 5. Structure–activity relationship of C(3)-substituted benzoxaboroles.



Compound	R2'	R4'	R3a	R3b	TBB IC <sub>50</sub> <sup>†</sup> (μg/ml) <sup>†</sup>	L929 IC <sub>50</sub> <sup>‡</sup> (μg/ml) <sup>‡</sup>	Mouse S9 metabolism (t <sub>1/2</sub> , min) <sup>§</sup>	logD	Solubility (μM) <sup>¶</sup>	Permeability <sup>#</sup>		In vivo, acute HAT model <sup>**</sup>	
										P <sub>app</sub> (nm/s)	P <sub>app</sub> +918 (nm/s)		AQ <sup>††</sup>
<b>27d</b>	H	F	CH <sub>3</sub>	H	0.05	>10	245	2.81	100	713	715	0.00	po (+)
<b>27f</b>	CF <sub>3</sub>	H	CH <sub>3</sub>	H	0.078	0.53	>350	2.93	3	569	604	0.06	
<b>27h</b>	Cl	H	CH <sub>3</sub>	H	0.024	1.24	>350	2.62	>200				po (+++)
<b>27i</b>	CF <sub>3</sub>	F	CH <sub>3</sub>	H	0.091	1.21	>350	3.20	50	683	707	0.03	
<b>27l (R)</b>	CF <sub>3</sub>	F	CH <sub>3</sub>	H	0.077	0.75							
<b>27l (S)</b>	CF <sub>3</sub>	F	CH <sub>3</sub>	H	0.554	>50							
<b>27m</b>	Cl	F	CH <sub>3</sub>	H	0.043	2	>350	2.88	>200				
<b>28f</b>	CF <sub>3</sub>	H	CH <sub>3</sub>	CH <sub>3</sub>	0.106	>10	>350	3.33	50	553	601		po (+++)
<b>28h</b>	Cl	H	CH <sub>3</sub>	CH <sub>3</sub>	0.168	>10	>350	3.18	13	859	884	0.03	po (+)
<b>28i</b>	CF <sub>3</sub>	F	CH <sub>3</sub>	CH <sub>3</sub>	0.292	>10	>350	3.51	25	415	427	0.03	po (+++)
<b>28m</b>	Cl	F	CH <sub>3</sub>	CH <sub>3</sub>	0.282	>10	>350	3.29	100				po (+++)
<b>29f</b>	CF <sub>3</sub>	H	Cyclopentyl	H	0.655	>10	68	4.39	25				
<b>30f</b>	CF <sub>3</sub>	H	Isobutyl	H	0.866	>10							

(+++)= active at 5 mg/kg; (++)= active at 10 mg/kg; (+)= active at 20 mg/kg; (-)= inactive at 20 mg/kg.

<sup>†</sup>Trypanocidal activity versus Trypanosoma brucei brucei S427.

<sup>‡</sup>Cytotoxicity versus L929 mouse fibroblasts.

<sup>§</sup>Stability in mouse S9 liver fraction.

<sup>¶</sup>Solubility in an MDCK-MDR1 cell monolayer assay.

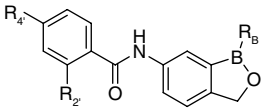
<sup>#</sup>Permeability in an MDCK-MDR1 cell monolayer assay.

<sup>\*\*</sup>[29].

<sup>††</sup>Activity in a stage 1 HAT model using mice infected with T. brucei EATRO 110 parasites [32].

AQ: Absorption quotient; HAT: Human African trypanosomiasis; P<sub>app</sub>: Apparent permeability; po: per os (oral) dosing; TBB: T. b. brucei.

Table 6. Structure–activity relationship of B-substituted benzoxaboroles.



Compound	RB	R2'	R4'	TBB IC <sub>50</sub> (µg/ml) <sup>†</sup>	L929 IC <sub>50</sub> (µg/ml) <sup>‡</sup>	Mouse S9 metabolism (t <sub>1/2</sub> ' min) <sup>§</sup>	Permeability <sup>¶</sup>			In vivo, acute HAT model <sup>††</sup>
							P <sub>app</sub> (nm/s)	P <sub>app</sub> +918 (nm/s)	AQ <sup>#</sup>	
<b>19f</b>	CH <sub>3</sub>	CF <sub>3</sub>	H	0.27	4.34	123	803	671	-0.20	
<b>20f</b>	vinyl	CF <sub>3</sub>	H	0.139	3.69	170	635	483	-0.32	
<b>21f</b>	Ph-	CF <sub>3</sub>	H	0.22	>10	61	866	469	-0.51	
<b>22f</b>	4-MePh-	CF <sub>3</sub>	H	0.22	>10	35	440	450	0.02	
<b>23f</b>	4-ClPh-	CF <sub>3</sub>	H	0.81	>10	147	445	400	-0.11	
<b>24f</b>	4-MeOPh-	CF <sub>3</sub>	H	0.125	>10	73	745	526	-0.42	
<b>25f</b>	4-Me <sub>2</sub> NPh	CF <sub>3</sub>	H	0.069	5.31	22				
<b>26f</b>	3,4-(MeO) <sub>2</sub> Ph	CF <sub>3</sub>	H	0.084	>10	47	1010	888	-0.14	po (-)
<b>24i</b>	4-MeOPh	CF <sub>3</sub>	F	0.089	>10	266				po (-)

(+++)= active at 5 mg/kg; (++)= active at 10 mg/kg; (+)= active at 20 mg/kg; (-)= inactive at 20 mg/kg.  
<sup>†</sup>Trypanocidal activity versus *Trypanosoma brucei* brucei S427.  
<sup>‡</sup>Cytotoxicity versus L929 mouse fibroblasts.  
<sup>§</sup>Stability in mouse S9 liver fraction.  
<sup>¶</sup>Permeability in an MDCK-MDR11 cell monolayer assay.  
<sup>#</sup>[29].  
<sup>††</sup>Activity in a stage 1 HAT model using mice infected with *T. brucei* EATRO 110 parasites [32].  
 AQ: Absorption quotient; HAT: Human African trypanosomiasis; P<sub>app</sub>: Apparent permeability; po: per os (oral) dosing; TBB: *T. b. brucei*.

Table 7. Efficacy of benzoxaborole 6-carboxamides in murine CNS human African trypanosomiasis model.

Entry	Compound	Dose (mg/kg)	Dose frequency	Dose route	Relapses <sup>†</sup>	Cured <sup>‡</sup>
1	<b>11f</b>	50	BID	ip <sup>§</sup>	1D49, 1D56	7/9 <sup>¶</sup>
2	<b>11h</b>	50	BID	ip <sup>§</sup>	1D105	8/9 <sup>¶</sup>
3	<b>11i</b>	50	BID	ip <sup>§</sup>		10/10
4	<b>11j</b>	50	BID	po	1D56	5/6 <sup>¶</sup>
5	<b>11k</b>	25	BID	po	5D34, 1D41, 2D48	2/10
6	<b>11l</b>	12.5	BID	po	7D34, 2D41, 1D48	0/10
7	<b>28f</b>	50	QD	po	2-D49	7/9 <sup>¶</sup>
8	<b>28h</b>	50	QD	po	7D35, 1D42	0/8 <sup>¶</sup>
9	<b>28i</b>	50	QD	po		9/9 <sup>¶</sup>
10	<b>28j</b>	25	QD	po		10/10
11	<b>28k</b>	12.5	QD	po	1D34, 1D48	8/10
12	<b>28l</b>	6	QD	po	6D34, 1D41, 3D48	0/10
13	<b>28m</b>	50	QD	po		9/9 <sup>¶</sup>
14	<b>28n</b>	25	QD	po	1D35, 3D42, 1D49	4/9 <sup>¶</sup>

<sup>†</sup>Relapses defined as appearance of parasites in blood obtained from a tail snip on day indicated.  
<sup>‡</sup>Defined as animals that remained parasite-free for 180 days post-infection.  
<sup>§</sup>Dosed for 14 days, all other groups dosed for 7 days starting on day 21 post-infection.  
<sup>¶</sup>Each experimental group started with ten mice. Mice found moribund prior to completion of the dosing period (7 or 14 days) were excluded from the study.  
 BID: Twice-daily dosing; ip: Interperitoneal dosing; po: per os (oral) dosing; QD: Once-daily dosing.

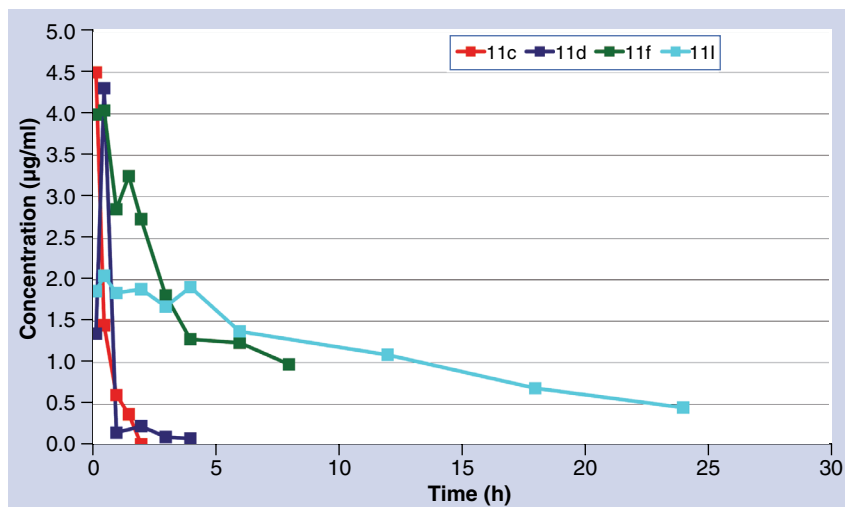


**Figure 6. Time versus plasma concentration curves for 11c, 11d, 11f and 11l following single nominal bolus intravenous dose of 2 mg/kg to mice (data normalized).** Male CD-1 mice were administered a single dose of test compound by intravenous injection. Blood samples were collected and analyzed by LC-MS/MS as described in [24]. Data points represent a single mouse at each time point.

Concurrent evaluation of the brain exposure of **III** in mice suggested that, while concentrations of drug were in excess of the minimum inhibitory concentration (MIC) for parasite growth (defined as the lowest concentration of compound that completely inhibits visible parasite growth determined by visual inspection of wells in the *in vitro* assay after 48–72 h of incubation, see [24]) at early (0–6 h) timepoints at therapeutic doses, drug levels dropped below the MIC by 12 h, which supported our decision to administer this compound in a twice-daily dosing (BID) regimen. We further characterized **III** in the stage 2 HAT model following oral administration at several doses (TABLE 7, entries 4–6). While efficacious when dosed at 50 mg/kg, BID for 7 days, lower doses (25, 12.5 or 6 mg/kg, BID  $\times$  7 days) were not effective. These observations prompted us to explore further variation of the 6-N series to attempt to improve potency and overcome the need for BID administration of drug compound.

Based on the improved efficacy in the stage 1 HAT model, several 3,3-disubstituted benzoxaboroles were also evaluated in the CNS model (TABLE 7, entries 7–14). In particular, **28i** was found to be very active in this model, where it was able to cure mice of CNS trypanosomes following once daily oral administration of 25 mg/kg for 7 days. The closely related analog **28m** was also efficacious in this model, albeit only at a once-daily oral dose of 50 mg/kg for 7 days. In contrast, **28f** and **28h** were not active at this

dose level, consistent with observations made for these compounds regarding duration of brain exposure in PK studies. Briefly, PK data suggest that efficacy in the CNS model is dependent upon maintenance of drug concentrations in the brain at or above the MIC for parasitocidal activity for at least 15 h to observe efficacy following once-daily administration of compound. In the case of compounds where brain concentrations fall more rapidly (e.g., **III**) cure of CNS infections can be achieved, but only after twice-daily administration of test compound. Interestingly, the data available to date suggest that total brain concentration correlated with efficacy to a greater extent than unbound (free) drug fraction – suggestive that binding to brain tissues is not restrictive, and that unbound compound rapidly traverses into parasites.

#### *In vivo* PKs

Key to our medicinal chemistry strategy was to integrate *in vivo* PK characterization of lead compounds concurrent with *in vivo* efficacy studies. This approach has not been widely used in previous programs for trypanocidal drugs due to limited resources available to those programs. Consequently, little information was available at the outset of our program as to which parameters (e.g.,  $C_{max}$ , AUC and  $t_{1/2}$ ) were important predictors of *in vivo* efficacy. Given the early lead-optimization stage of the program and a desire to minimize numbers of animals used, our strategy was to utilize a fit-for-purpose discovery *in vivo* PK screening paradigm that used one mouse per timepoint. While this approach is not designed to provide definitive PK parameters for a compound, nor enable fine discrimination between the PK of closely related compounds, we have found it useful to distinguish classes of compounds with attractive properties from those that do not meet requirements for progression to more labor intensive models. One practical consequence of this approach is the potential for observation of multiple  $C_{max}$  values (such as was observed for **28i**), most likely due to variability in dosing of individual animals.

Early representatives of the oxaborole 6-carboxamides (**11c**, **11d** & **11f**) exhibited modest *in vivo* PK following intravenous dosing (FIGURE 6), with both  $C_{max}$  and  $t_{1/2}$  broadly reflective of *in vitro* metabolic stability. Improvement of metabolic stability, as in **III**, was accompanied by concomitant improvements in plasma PK.

#### Key Term

**Trypanosomes:** Monocellular, flagellate protozoan parasites of the class Kinetoplastida that includes *Trypanosoma brucei*, the causative agent of human African trypanosomiasis.

Modest to good plasma PK was also observed following oral dosing for representatives of the 3-monosubstituted benzoxaboroles (**27l** & **27m**) and 3,3-disubstituted benzoxaboroles (**28l** & **28m**) as shown in **FIGURE 7**. Direct comparisons between these subseries (e.g., **11l** vs **27l** vs **28l**, and **11m** vs **27m** vs **28m**) suggested that the 3,3-dimethyl analogs were generally better than the 3,3-unsubstituted and 3-monosubstituted analogs, which, when combined with the somewhat lower *in vitro* potency of the 3,3-disubstituted analogs, resulted in relatively similar potencies of these compounds in the murine stage 1 HAT model.

In comparison, we found that it was much more difficult to achieve high brain concentrations for extended periods, despite the *in vitro* MDCK-MDR1 data, which predicted most of the benzoxaborole 6-carboxamides to be highly permeable and of limited affinity for the Pgp transporter. In particular, the 3,3-unsubstituted (**11l** & **11m**) and 3-monosubstituted (**27l** & **27m**) analogs were present at therapeutically relevant levels (e.g., concentrations >MIC) in brain for only short periods (e.g.,  $t < 6$  h), whereas the 3,3-dimethyl analogs (**28l** & **28m**) were much more long-lived in the brain (e.g.,  $t$  above MIC >12 h) as depicted in **FIGURE 8**. These trends in brain PK were consistent with observations in the CNS efficacy model, where the 3,3-dimethyl compounds were active following once-daily dosing, and some of the 3,3-unsubstituted analogs were active only when dosed twice daily.

## Conclusions

Benzoxaboroles have been identified that exhibit potent trypanocidal activity against the causative agent of HAT, *T. brucei*. Following identification of lead compounds in an *in vitro* whole-cell assay, expansion of the series allowed us to focus on a series of 6-carboxamides, which have been found to have physicochemical and ADME properties predictive of activity in animal models of HAT. This activity has been confirmed in both stage 1 and stage 2 HAT murine models, and data for the relationship between PK behavior and *in vivo* efficacy has been presented. SAR of the series has highlighted 3,3-disubstituted benzoxaborole 6-carboxamides, exemplified by **28l** and **28m**, as promising agents for the treatment of stage 2 HAT, as these compounds have been found to cure mice infected with trypanosomes resident in brain tissue. Significant work remains, particularly in development of a greater understanding of the PK-pharmacodynamic

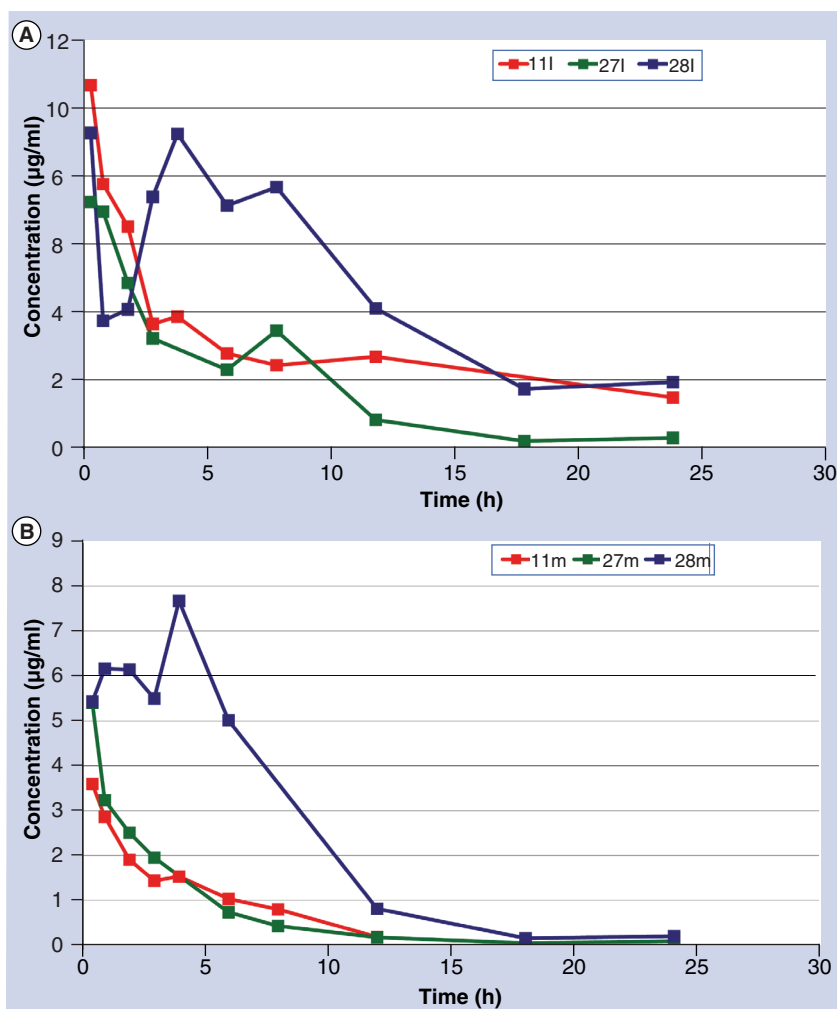


**Figure 7. Time versus plasma concentration curves for compounds following oral administration to mice. (A)** Data for 2-trifluoromethyl-4-fluorobenzamide analogs **11l**, **27l** and **28l**. **(B)** Data for 2-chloro-4-fluorobenzamide analogs **11m**, **27m** and **28m**. Male CD-1 mice were administered a single dose of test compound by oral gavage. Blood samples were collected and analyzed by LC-MS/MS as described in [24]. Data points represent a single mouse at each time point.

relationship for this class of compounds in this disease, and in characterization of the toxicological and pharmaceutical properties of lead compounds such as **28l** prior to progression to clinical trials [35].

## Future perspective

Only recently have compounds containing a boron atom been explored in a concerted and systematic manner. Many of the concerns initially raised about organoboron pharmaceuticals, such as chemical reactivity and resultant toxicity, have been diminished through the delivery of the cyclized oxaborole scaffolds. With several compounds from this class currently in, or about to enter, clinical trials, many

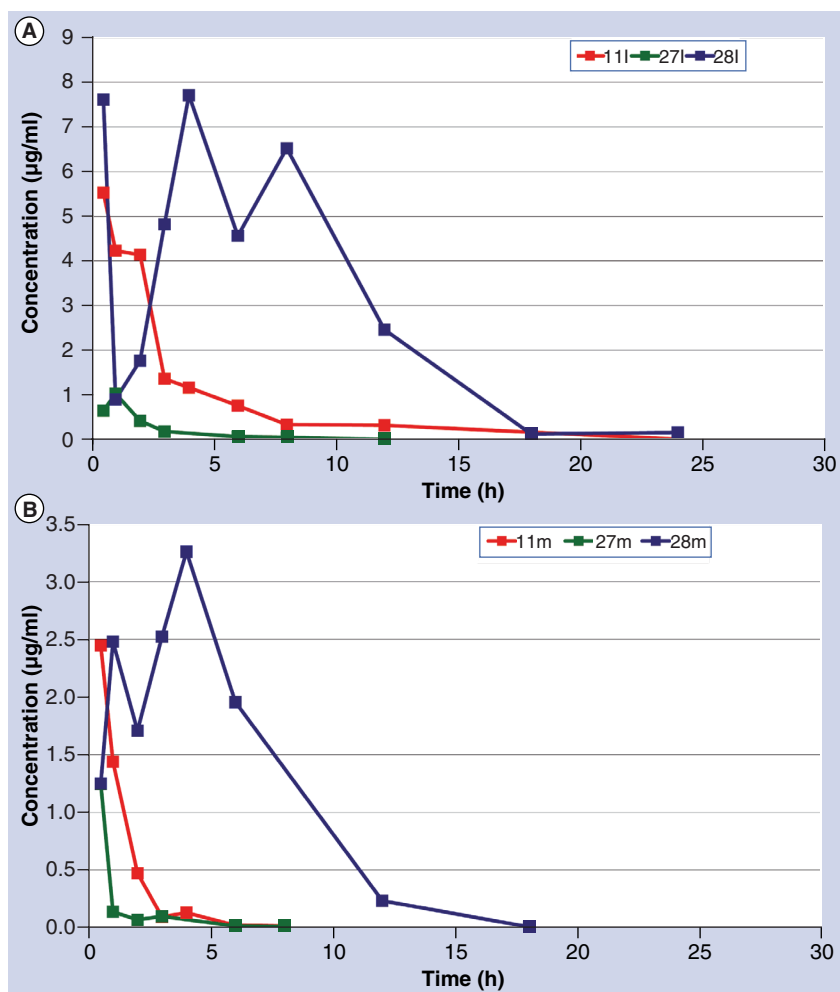


**Figure 8. Time versus brain concentration curves for compounds following oral administration to mice. (A)** Data for 2-trifluoromethyl-4-fluorobenzamide analogs **111**, **271** and **281**. **(B)** Data for 2-chloro-4-fluorobenzamide analogs **11m**, **27m** and **28m**. Male CD-1 mice were administered a single dose of test compound by oral gavage. Blood samples were collected and analyzed by LC-MS/MS as described in [24]. Data points represent a single mouse at each time point.

of the questions around potential for long-term effects or toxicity will be answered in the next few years. If successful, the addition of boron-containing compounds to the arsenal of potential drug candidates will expand opportunities in anti-infective and other disease areas.

In the area of neglected tropical diseases, historical efforts have been characterized to a large degree by empirical screening of known cytotoxic or antimicrobial compounds in whole-cell parasitocidal assays, followed by *in vivo* evaluation at arbitrarily chosen doses with little effort expended on understanding the role of PKs on *in vivo* activity. The research project described here is, to our knowledge, the first fully integrated drug-discovery project focused on HAT.

In the relatively short time we have spent in this field, we have made significant progress in development of our understanding of the PK–PD relationship for the oxaboroles and treatment of HAT. Application of this paradigm to other compound classes, and to other neglected tropical diseases, may provide a cost-efficient avenue to the discovery of new treatments for these devastating diseases.

### Acknowledgements

The authors thank Tana Bowling, Luke Mercer, Ryan Randolph, Cindy Rewerts and Jennifer Owens (SCYNEXIS), and Aixa Rodriguez, Ali Hussain, Elena Mejia, Wendy Becker and Donna Rattendi (Pace University) for expert technical assistance. We also thank Reto Brun and Marcel Kaiser (Swiss Tropical and Public Health Institute) for provision of *in vitro* data for *Trypanosoma brucei rhodesiense* and *Trypanosoma brucei gambiense* strains, and Alan Hudson and Tom von Geldern (independent consultants) for helpful discussions throughout this project.

### Ethical conduct of research

The authors state that they have obtained appropriate institutional review board approval or have followed the principles outlined in the Declaration of Helsinki for all human or animal experimental investigations.

### Financial & competing interests disclosure

Robert T Jacobs, Bakela Nare, Stephen A Wring, Daitao Chen, Eric G Gaukel, Matthew D Orr, Joe B Perales, Matthew Jenks, Robert A Noe and Jessica M Sligar are employees of SCYNEXIS, Inc. Jacob J Plattner, Yvonne Freund and Yong-Kang Zhang are employees of Anacor Pharmaceuticals, Cyrus J Bacchi and Nigel Yarlett are employees of Pace University. Robert Don is an employee of the Drugs for Neglected Diseases Initiative.

The following sources have provided funding for this work: the Bill & Melinda Gates Foundation (Grant number OPP48262), the Department for International Development (UK), Médecins Sans Frontières International and the Spanish Agency of International Cooperation and Development. The authors have no other relevant affiliations or financial involvement with any organization or entity with a financial interest in or financial conflict with the subject matter or materials discussed in this manuscript. No writing assistance was utilized in the production of this manuscript.

### Supplementary data

To view the supplementary data that accompany this paper please visit the journal website at: [www.future-science.com/doi/suppl/10.4155/FMC.11.80](http://www.future-science.com/doi/suppl/10.4155/FMC.11.80).

## Executive summary

- Human African trypanosomiasis (HAT) is a significant health problem in sub-Saharan Africa, with tens of thousands of victims each year.
- Treatment options for stage 2 HAT, where parasites have crossed the blood–brain barrier, are particularly problematic due to toxicity and difficulty of administration.
- Benzoxaborole-6-carboxamides (e.g., **11**) have been discovered with potent *in vitro* trypanocidal activity against *Trypanosoma brucei*, with little evidence of cytotoxicity to mammalian cells.
- Integration of *in vitro* ADME evaluation of early leads facilitated selection of compounds for progression into an *in vivo* model where efficacy was demonstrated.
- Replacement of the carboxamide function with sulfonamide, urea or carbamate retained *in vitro* trypanocidal activity, but negatively impacted *in vitro* ADME properties.
- Optimization of the benzoxaborole-6-carboxamides through systematic exploration of substitution of the benzamide moiety and benzoxaborole core afforded compounds (e.g., **28**) with significantly improved ADME properties.
- Concurrent evaluation of lead compounds in both *in vivo* efficacy and PK models provided a rationale for selection of compounds to progress to a murine model of stage 2 HAT.
- Optimized lead compounds (**28i & 28m**) were found to be efficacious in the murine stage 2 HAT model after oral administration of 25 mg/kg/day and 50 mg/kg/day for 7 days, respectively.
- A preliminary relationship between concentration of compound in brain tissue and efficacy has been observed, with work to further refine understanding this relationship in progress.
- Compound **28i** (SCYX-7158) has been selected for further evaluation as a preclinical candidate for treatment of stage 2 HAT.

## Bibliography

Papers of special note have been highlighted as:

▪ of interest

▪▪ of considerable interest

- 1 WHO. Human African trypanosomiasis (sleeping sickness): epidemiological update. *Wkly Epidemiol. Rec.* 81(8), 71–80 (2006).
- 2 Simarro PP, Jannin J, Cattand P. Eliminating human African trypanosomiasis: where do we stand and what comes next? *PLoS Med.* 5(2), e55 (2008).
- 3 Fèvre EM, Wissmann BV, Welburn SC, Lutumba P. The burden of human African trypanosomiasis. *PLoS Negl. Trop. Dis.* 2(12), e333 (2008).
- 4 Grab DJ, Kennedy PG. Traversal of human and animal trypanosomes across the blood–brain barrier. *J. Neurovirol.* 14(5), 344–351 (2008).
- 5 Wilkinson SR, Kelly JM. Trypanocidal drugs: mechanisms, resistance and new targets. *Expert Rev. Mol. Med.* 11, e31 (2009).
- **Recent review of strategies for discovery of new therapeutic agents to treat human African trypanosomiasis.**
- 6 Croft SL, Barrett MP, Urbina JA. Chemotherapy of trypanosomiasis and leishmaniasis. *Trends Parasitol.* 21(11), 508–512 (2005).
- 7 Mccann PP, Bitonti AJ, Bacchi CJ, Clarkson AB Jr. Use of difluoromethylornithine (DFMO, eflornithine) for late-stage African trypanosomiasis. *Trans. R. Soc. Trop. Med. Hyg.* 81(4), 701–702 (1987).
- 8 Priotto G, Kasparian S, Nguouama D *et al.* Nifurtimox–eflornithine combination therapy for second-stage *Trypanosoma brucei* gambiense sleeping sickness: a randomized clinical trial in Congo. *Clin. Infect. Dis.* 45(11), 1435–1442 (2007).
- 9 Checchi F, Piola P, Ayikoru H, Thomas F, Legros D, Priotto G. Nifurtimox plus Eflornithine for late-stage sleeping sickness in Uganda: a case series. *PLoS Negl. Trop. Dis.* 1(2), e64 (2007).
- 10 Priotto G, Kasparian S, Mutombo W *et al.* Nifurtimox–eflornithine combination therapy for second-stage African *Trypanosoma brucei* gambiense trypanosomiasis: a multicentre, randomised, phase III, non-inferiority trial. *Lancet* 374(9683), 56–64 (2009).
- **Description of the pivotal phase III clinical trial, which demonstrated utility of the nifurtimox–eflornithine combination therapy for stage 2 sleeping sickness.**
- 11 Yun O, Priotto G, Tong J, Flevaud L, Chappuis F. NECT is next: implementing the new drug combination therapy for *Trypanosoma brucei* gambiense sleeping sickness. *PLoS Negl. Trop. Dis.* 4(5), e720 (2010).
- 12 Philipp M, Bender ML. Inhibition of serine proteases by arylboronic acids. *Proc. Natl Acad. Sci. USA* 68(2), 478–480 (1971).
- 13 Groziak MP. Boron therapeutics on the horizon. *Am. J. Ther.* 8(5), 321–328 (2001).
- 14 Trippier PC, Mcguigan C. Boronic acids in medicinal chemistry: anticancer, antibacterial and antiviral applications. *MedChemComm* 1(3), 183–198 (2010).
- 15 Baker SJ, Tomsho JW, Benkovic SJ. Boron-containing inhibitors of synthetases. *Chem. Soc. Rev.* (2011).
- **Recent review of boron-containing drug candidates including benzoxaboroles.**
- 16 Baker SJ, Zhang YK, Akama T *et al.* Discovery of a new boron-containing antifungal agent, 5-fluoro-1,3-dihydro-1-hydroxy-2,1-benzoxaborole (AN2690), for the potential treatment of onychomycosis. *J. Med. Chem.* 49(15), 4447–4450 (2006).
- 17 Rock FL, Mao W, Yaremchuk A *et al.* An antifungal agent inhibits an aminoacyl-tRNA synthetase by trapping tRNA in the editing site. *Science* 316(5832), 1759–1761 (2007).
- **Describes the structural basis for inhibition of the aminoacyl-tRNA synthetase by covalent interaction of a benzoxaborole with the ribose moiety of ATP.**
- 18 Xia Y, Cao K, Zhou Y *et al.* Synthesis and SAR of novel benzoxaboroles as a new class of  $\beta$ -lactamase inhibitors. *Bioorg. Med. Chem. Lett.* 21(8), 2533–2536 (2011).
- 19 Akama T, Baker SJ, Zhang YK *et al.* Discovery and structure–activity study of a novel benzoxaborole anti-inflammatory agent (AN2728) for the potential topical treatment of psoriasis and atopic dermatitis. *Bioorg. Med. Chem. Lett.* 19(8), 2129–2132 (2009).
- 20 Hernandez V, Akama T, Alley MR *et al.* Discovery and mechanism of action of an3365: a novel boron containing antibacterial agent in clinical development for Gram-negative infections. Presented at: 50th

- Interscience Conference on Antimicrobial Agents and Chemotherapy (ICAAC)*. Boston, MA, USA, 12–15 September 2010.
- 21 Zhang YK, Plattner JJ, Freund YR *et al.* Synthesis and structure–activity relationships of novel benzoxaboroles as a new class of antimalarial agents. *Bioorg. Med. Chem. Lett.* 21(2), 644–651 (2011).
  - 22 Li X, Zhang YK, Liu Y *et al.* Synthesis of new acylsulfamoyl benzoxaboroles as potent inhibitors of HCV NS3 protease. *Bioorg. Med. Chem. Lett.* 20(24), 7493–7497 (2010).
  - 23 Ding CZ, Zhang YK, Li X *et al.* Synthesis and biological evaluations of P4-benzoxaborole-substituted macrocyclic inhibitors of HCV NS3 protease. *Bioorg. Med. Chem. Lett.* 20(24), 7317–7322 (2010).
  - 24 Nare B, Wring S, Bacchi C *et al.* Discovery of novel orally bioavailable oxaborole 6-carboxamides that demonstrate cure in a murine model of late-stage central nervous system African trypanosomiasis. *Antimicrob. Agents Chemother.* 54(10), 4379–4388 (2010).
  - **Important article that describes in detail the biological and PK properties of early benzoxaborole-6-carboxamides.**
  - 25 Ding D, Zhao Y, Meng Q *et al.* Discovery of novel benzoxaborole-based potent antitrypanosomal agents. *ACS Med. Chem. Lett.* 1(4), 165–169 (2010).
  - **Describes initial efforts in the benzoxaborole series following high-throughput screening of the Anacor Pharmaceuticals compound library.**
  - 26 Lipinski CA. Drug-like properties and the causes of poor solubility and poor permeability. *J. Pharmacol. Toxicol. Methods* 44(1), 235–249 (2000).
  - 27 Lipinski CA, Lombardo F, Dominy BW, Feeney PJ. Experimental and computational approaches to estimate solubility and permeability in drug discovery and development. *Adv. Drug Delivery Rev.* 23(1–3), 3–25 (1997).
  - 28 Mahar Doan KM, Wring SA, Shampine LJ *et al.* Steady-state brain concentrations of antihistamines in rats: interplay of membrane permeability, P-glycoprotein efflux and plasma protein binding. *Pharmacology* 72(2), 92–98 (2004).
  - 29 Thiel-Demby VE, Tippin TK, Humphreys JE, Serabjit-Singh CJ, Polli JW. *In vitro* absorption and secretory quotients: practical criteria derived from a study of 331 compounds to assess for the impact of P-glycoprotein-mediated efflux on drug candidates. *J. Pharm. Sci.* 93(10), 2567–2572 (2004).
  - 30 Brun R, Baeriswyl S, Kunz C. *In vitro* drug sensitivity of *Trypanosoma gambiense* isolates. *Acta Trop.* 46(5–6), 369–376 (1989).
  - 31 Likeufack AC, Brun R, Fomena A, Truc P. Comparison of the *in vitro* drug sensitivity of *Trypanosoma brucei gambiense* strains from West and Central Africa isolated in the periods 1960–1995 and 1999–2004. *Acta Trop.* 100(1–2), 11–16 (2006).
  - 32 Bacchi CJ, Brun R, Croft SL, Alicea K, Buhler Y. *In vivo* trypanocidal activities of new *S*-adenosylmethionine decarboxylase inhibitors. *Antimicrob. Agents Chemother.* 40(6), 1448–1453 (1996).
  - 33 Jennings FW, Gray GD. Relapsed parasitaemia following chemotherapy of chronic *T. brucei* infections in mice and its relation to cerebral trypanosomes. *Contrib. Microbiol. Immunol.* 7, 147–154 (1983).
  - 34 Bacchi CJ, Nathan HC, Clarkson AB Jr *et al.* Effects of the ornithine decarboxylase inhibitors DL- $\alpha$ -difluoromethylornithine and  $\alpha$ -monofluoromethyldehydroornithine methyl ester alone and in combination with suramin against *Trypanosoma brucei brucei* central nervous system models. *Am. J. Trop. Med. Hyg.* 36(1), 46–52 (1987).
  - 35 Jacobs RT, Nare B, Wring SA *et al.* SCYX-7158, an orally-active benzoxaborole for the treatment of stage 2 human African trypanosomiasis. *PLoS Negl. Trop. Dis.* 5(6), e1151 (2011).